

Sharp Analysis of Sketch-and-Project Methods via a Connection to Randomized Singular Value Decomposition

Michał Dereziński* and Elizaveta Rebrova†

Abstract

Sketch-and-project is a framework which unifies many known iterative methods for solving linear systems and their variants, as well as further extensions to non-linear optimization problems. It includes popular methods such as randomized Kaczmarz, coordinate descent, variants of the Newton method in convex optimization, and others. In this paper, we obtain sharp guarantees for the convergence rate of sketch-and-project methods via new tight spectral bounds for the expected sketched projection matrix. Our estimates reveal a connection between the sketch-and-project convergence rate and the approximation error of another well-known but seemingly unrelated family of algorithms, which use sketching to accelerate popular matrix factorizations such as QR and SVD. This connection brings us closer to precisely quantifying how the performance of sketch-and-project solvers depends on their sketch size. Our analysis covers not only Gaussian and sub-gaussian sketching matrices, but also a family of efficient sparse sketching methods known as LESS embeddings. Our experiments back up the theory and demonstrate that even extremely sparse sketches show the same convergence properties in practice.

1 Introduction

Randomized sketching is one of the most popular dimension-reduction techniques, applied in a variety of linear algebra, compressed sensing, and machine learning tasks [Woo14, HMRT19, MT20, DM21]. From linear regression to computing singular value decomposition, multiplying the data by a random matrix can reduce the size of the problem while preserving its important characteristics. Prototypical examples of sketching matrices are Gaussian matrices with independent entries and other matrices satisfying the Johnson-Lindenstrauss property (preserving the geometry of the data), or block-identity matrices that effectively subsample the data matrix. A variety of other sketching matrices have been proposed [AC09, CW17, NN13, DLDM21], seeking the trade-off between the complexity of the model, its storage requirements, its effectiveness in compressing the data, and the cost of sketching.

One important application of sketching is to construct a random low-dimensional subspace, such that much of the information contained in the data is retained after projecting onto this subspace. This use case arises primarily in two algorithmic paradigms: (1) as part of an iterative solver which performs the sketching repeatedly, gradually converging to the desired solution (known as *sketch-and-project*); and (2) as a basis for an approximate matrix factorization algorithm where the sketching is performed once (we refer to this as *Randomized SVD*). Traditionally, these two paradigms have been studied independently, due to very different performance metrics. Yet, in this work, while our primary goal is to characterize the convergence

*derezin@umich.edu, Department of Electrical Engineering and Computer Science, University of Michigan.

†elre@princeton.edu, Department of Operations Research and Financial Engineering, Princeton University. ER was partially supported by NSF DMS 2108479.

rates of iterative solvers based on sketch-and-project, we show that a crucial part of this characterization is a new connection with the approximation error in Randomized SVD. We start by briefly introducing both of the algorithmic paradigms.

Sketch-and-project. This method was developed as a unified framework for iteratively solving linear systems [GR15], although it can be directly extended to non-linear optimization problems (see Section 3). For concreteness, let us consider our key application, projection-based linear solvers for overdetermined systems, aiming to find \mathbf{x} that satisfies $\mathbf{A}\mathbf{x} = \mathbf{b}$ for $\mathbf{A} \in \mathbb{R}^{m \times n}$ and $\mathbf{b} \in \mathbb{R}^m$. Instead of projecting directly onto the range of \mathbf{A} to find $\mathbf{x}_* = \mathbf{A}^\dagger \mathbf{b}$, one can consider iterative projections on the ranges of smaller *sketched* matrices $\mathbf{S}\mathbf{A}$ where $\mathbf{S} \in \mathbb{R}^{k \times m}$ with $k \ll n \leq m$. It is important that the distribution of all sketching matrices \mathbf{S} is such that individual realizations of $\mathbf{S}\mathbf{A}$ cover the full range of the matrix \mathbf{A} . Then, for $t = 0, 1, \dots$ a random sketching matrix $\mathbf{S} = \mathbf{S}(t)$ is sampled from such distribution and the update rule is given by

$$\mathbf{x}_{t+1} = \operatorname{argmin}_{\mathbf{x} \in \mathbb{R}^n} \|\mathbf{x}_t - \mathbf{x}\|_{\mathbf{B}}^2 \quad \text{such that} \quad \mathbf{S}\mathbf{A}\mathbf{x} = \mathbf{S}\mathbf{b}. \quad (1)$$

This optimization problem can be solved directly and is equivalent to an iterative step

$$\mathbf{x}_{t+1} = \mathbf{x}_t - \mathbf{B}^{-1} \mathbf{A}^\top \mathbf{S}^\top (\mathbf{S}\mathbf{A}\mathbf{B}^{-1} \mathbf{A}^\top \mathbf{S}^\top)^\dagger \mathbf{S} (\mathbf{A}\mathbf{x}_t - \mathbf{b}).$$

Here, $(\cdot)^\dagger$ denotes the Moore-Penrose pseudoinverse and the positive definite matrix \mathbf{B} defines the projection operator. For example, $\mathbf{B} = \mathbf{I}$ defines the usual Euclidean projection. Varying the \mathbf{S} and \mathbf{B} matrices (i.e., the ways to sketch and to project), this general update rule reduces to randomized Gaussian pursuit, Randomized Kaczmarz, and Randomized Newton methods, among others [GR15, GKLR19]. The performance of these methods is often measured through the worst-case expected convergence rate:

$$\operatorname{Rate}_{\mathbf{B}}(\mathbf{A}, k) := \sup \left\{ \rho \text{ s.t. } \mathbb{E} \|\mathbf{x}_t - \mathbf{x}_*\|_{\mathbf{B}}^2 \leq (1 - \rho)^t \cdot \|\mathbf{x}_0 - \mathbf{x}_*\|_{\mathbf{B}}^2 \quad \forall \mathbf{x}_0, t \right\}. \quad (2)$$

Randomized SVD. This is a family of methods which use a randomized subspace generated from a sketch of the input matrix to accelerate performing restricted versions of matrix factorizations such as QR and SVD [HMRT19] (we focus on SVD for the sake of concreteness). When the sketch is based on a block identity matrix, then this approach is also known as Column/Row Subset Selection [BMD08]. These methods use a two-stage procedure.

1. First, one finds an approximate basis for the row-span of a target matrix \mathbf{A} , i.e., an $n \times k$ matrix \mathbf{Q} with orthonormal columns such that $\mathbf{A} \approx \mathbf{A}\mathbf{Q}\mathbf{Q}^\top$. This task, also known as the rangefinder problem, can be accomplished by generating a sketch $\mathbf{S}\mathbf{A}$ of size k , and then letting \mathbf{Q} be the orthonormal basis for the row-span of $\mathbf{S}\mathbf{A}$.
2. Next, one uses \mathbf{Q} to help compute a factorization of \mathbf{A} . For example, to obtain an approximate SVD with this procedure, i.e., $\mathbf{A} \approx \mathbf{U}\Sigma\mathbf{V}^\top$, we can compute an SVD of the small matrix $\mathbf{A}\mathbf{Q}$, letting $\mathbf{A}\mathbf{Q} = \mathbf{U}\Sigma\tilde{\mathbf{V}}^\top$, and then set $\mathbf{V} = \mathbf{Q}\tilde{\mathbf{V}}$.

It is important that the number of columns in \mathbf{Q} (i.e., the sketch size k) is small, as that reduces the computational cost of the second step. While there are many factorization algorithms that can be applied to this paradigm, the effectiveness of this approach is limited by the approximation error of the random orthonormal basis \mathbf{Q} . One common way to measure this error is via the expected Frobenius norm¹ of the residual after projecting onto the subspace defined by the basis (e.g., see [BMD08, HMRT19]):

$$\operatorname{Err}(\mathbf{A}, k) := \mathbb{E} \|\mathbf{A} - \mathbf{A}\mathbf{Q}\mathbf{Q}^\top\|_F^2 = \mathbb{E} \|\mathbf{A}(\mathbf{I} - \mathbf{A}^\top \mathbf{S}^\top (\mathbf{S}\mathbf{A}\mathbf{A}^\top \mathbf{S}^\top)^\dagger \mathbf{S}\mathbf{A})\|_F^2, \quad (3)$$

¹The spectral norm is also standard, but the Frobenius norm best suits our analysis of sketch-and-project.

where $\mathbf{Q}\mathbf{Q}^\top = \mathbf{A}^\top \mathbf{S}^\top (\mathbf{S}\mathbf{A}\mathbf{A}^\top \mathbf{S}^\top)^\dagger \mathbf{S}\mathbf{A}$ is the sketched projection matrix which is central to our analysis of sketch-and-project.

1.1 Contributions

Connection between sketch-and-project and Randomized SVD. While there are numerous differences in the above two algorithmic paradigms, the key aspect they have in common is that their performance depends on how much information is retained in the input matrix after it is projected onto the subspace defined by the sketch.

In this paper, we make this intuition concrete by relating their performance metrics. At a high-level, our theoretical results show that when the sketching matrix \mathbf{S} exhibits a sufficiently Gaussian-like distribution, then:

$$\text{Rate}_{\mathbf{B}}(\mathbf{A}, k) \gtrsim \frac{k \cdot \sigma_{\min}^2(\tilde{\mathbf{A}})}{\text{Err}(\tilde{\mathbf{A}}, k-1)} \quad \text{for} \quad \tilde{\mathbf{A}} = \mathbf{A}\mathbf{B}^{-1/2}, \quad (4)$$

where $\sigma_{\min}(\cdot)$ denotes the smallest singular value of a matrix, and recall from (2) that larger $\text{Rate}_{\mathbf{B}}(\mathbf{A}, k)$ means faster convergence. When $\mathbf{B} = \mathbf{I}$, which is the most common setup, then $\tilde{\mathbf{A}} = \mathbf{A}$ and our bound on the convergence rate of sketch-and-project is inversely proportional to the error of Randomized SVD applied on the same input matrix. This aligns with the intuition that the iterations of the solver, being constrained to the subspace, are more precise for the whole system, and thus lead to a better convergence rate, when the subspace approximation error is smaller. While the above informal statement is hiding a constant factor in the bound, we show that, under a variety of sketching distributions \mathbf{S} and for a wide range of sketch sizes k , the bound can be shown with a multiplicative factor $1 - o(1)$, i.e., approaching 1 asymptotically.

Better rate estimates for sketch-and-project. Our new convergence bound provides the sharpest known rate estimate for the sketch-and-project method. In the case when $\mathbf{B} = \mathbf{I}$ and $k = 1$, we recover the standard convergence guarantee for Randomized Kaczmarz [SV09], i.e., $\text{Rate}(\mathbf{A}, 1) \gtrsim \sigma_{\min}^2(\mathbf{A})/\|\mathbf{A}\|_F^2$, since $\text{Err}(\mathbf{A}, 0) = \|\mathbf{A}\|_F^2$. When we start increasing the sketch size k , our convergence rate bound improves at least linearly with k , since $\text{Err}(\mathbf{A}, k)$ is a non-increasing function in k . This aligns with prior analysis [RN21] for the so-called Block Gaussian Kaczmarz, where $\mathbf{B} = \mathbf{I}$ and \mathbf{S} is Gaussian, while also improving their bounds (see Section 3.1).

In addition, our results show that if the Randomized SVD error decreases rapidly with k , which occurs when \mathbf{A} exhibits fast spectral decay, then the convergence rate of sketch-and-project improves *superlinearly*² with k . And if the Randomized SVD error decrease exhibits an abrupt change at a certain value of k , that value suggests a viable sketch size for an effective convergence of sketch-and-project. This aligns with the intuition that if the effective rank of the data matrix is $k \ll n$ then a good k -dimensional sketch will contain essentially all information about the data, and the solution of the sketched system will nearly coincide with the true solution \mathbf{x}_* . Thus, the new rate estimates significantly advance our understanding of the quantitative effect that the sketch size has on the convergence, both for general data matrices, and even more so under additional spectral decay assumptions (see Corollary 1 for a summary).

Our unified characterization of the convergence rate can also be applied to other randomized algorithms based on the sketch-and-project framework, including non-linear system solvers [YLG22], iterative matrix inversion [GR17], and certain stochastic Newton methods for convex optimization [GKLR19] (see Section 2.4).

²For example, in combination with existing bounds for the Randomized SVD error, we show that, when the input matrix \mathbf{A} exhibits polynomial spectral decay with $\sigma_i^2(\mathbf{A}) \asymp i^{-\beta}$ for $\beta > 1$, then Block Gaussian Kaczmarz exhibits convergence with $\text{Rate}(\mathbf{A}, k) \gtrsim k^\beta \sigma_{\min}^2(\mathbf{A})/\|\mathbf{A}\|_F^2$ (see Corollary 1).

Spectral analysis of expected projection matrix. As a starting point, our analysis of sketch-and-project uses a known characterization of its convergence rate in terms of the smallest eigenvalue of the expected projection onto the random subspace defined by the sketch [GR15]:

$$\text{Rate}_{\mathbf{B}}(\mathbf{A}, k) \geq \lambda_{\min}(\mathbb{E}[\mathbf{P}]) \quad \text{for} \quad \mathbf{P} := \tilde{\mathbf{A}}^\top \mathbf{S}^\top (\mathbf{S} \tilde{\mathbf{A}} \tilde{\mathbf{A}}^\top \mathbf{S}^\top)^\dagger \tilde{\mathbf{S}} \tilde{\mathbf{A}}, \quad (5)$$

where $\tilde{\mathbf{A}} = \mathbf{A}\mathbf{B}^{-1/2}$. Thus, lower bounding the smallest eigenvalue of $\mathbb{E}[\mathbf{P}]$ immediately implies a convergence guarantee for sketch-and-project. Yet, spectral analysis of the expected projection matrix has proven challenging for most sketching distributions, even such common ones as the Gaussian sketch. Thus, our main technical contribution is a sharp spectral analysis of the expected projection, that goes even beyond its smallest eigenvalue, for Gaussian, sub-gaussian and sparse sketching matrices.

The key technical part of our analysis is a careful decomposition of the projection matrix \mathbf{P} via rank-one update formulas, and utilizing concentration of random quadratic forms based on the Hanson-Wright inequality. The connection to Randomized SVD error comes from the fact that this error can also be expressed as a function of the expected projection matrix, namely, $\text{Err}(\tilde{\mathbf{A}}, k) = \text{tr} \tilde{\mathbf{A}}^\top \tilde{\mathbf{A}} (\mathbf{I} - \mathbb{E}[\mathbf{P}])$, and this function naturally arises in our analysis. We remark that our proof in the Gaussian case (Theorem 1) relies on a completely different decomposition of \mathbf{P} than our full-spectrum analysis for general sub-gaussian sketches (Theorem 2), which is why the former applies to a broader range of sketch sizes and input matrices, whereas the latter applies to a wider family of sketching distributions.

We give all formal statements of the main results in Section 2. In summary:

1. We give a lower bound on the smallest eigenvalue $\lambda_{\min}(\mathbb{E}[\mathbf{P}])$ under the assumption that the sketching matrix has Gaussian entries, and translate it to convergence rate guarantees for sketch-and-project. We show that the rate improves at least linearly with the sketch size k , and faster (in terms of k) for matrices \mathbf{A} with certain spectral decays (Section 2.1).
2. We give full-spectrum two-sided estimates for the matrix $\mathbb{E}[\mathbf{P}]$, when sketch size k is smaller than the stable rank of the matrix \mathbf{A} . These guarantees are shown for a wider range of sketching distributions that satisfy certain concentration of measure properties, including matrices with i.i.d. sub-gaussian entries. (Section 2.2).
3. We then show that even certain very sparse sketching matrices, known as Leverage Score Sparsified (LESS) embeddings, are covered by our full-spectrum analysis of the expected projection. These sketches can be implemented much more efficiently than dense Gaussian or sub-gaussian matrices, resulting in a substantially lower per-iteration cost of sketch-and-project (Section 2.3).
4. Finally, we show that our convergence analysis can be easily extended to certain stochastic Newton methods in convex optimization. Here, sketching is applied to the Newton system that arises at each step of the optimization, and the convergence is characterized via the spectral properties of the Hessian of the objective (Section 2.4).

Empirical results show that our theoretical predictions for the performance of sketch-and-project are very accurate and extend even beyond these settings.

1.2 Notation and outline

We use \mathbf{a}_i^\top and $\sigma_i(\mathbf{A})$ to denote the i th row and i th largest singular value of matrix \mathbf{A} , while \mathbf{A}^\dagger denotes the Moore-Penrose pseudoinverse. Also, $\|\mathbf{A}\|$, $\|\mathbf{A}\|_F$ and $\|\mathbf{A}\|_*$ are the spectral/operator, Frobenius/Hilbert-Schmidt and trace/nuclear norms, respectively. For positive semidefinite matrices \mathbf{B} and \mathbf{C} , we use $\mathbf{B} \leq \mathbf{C}$ to denote the Loewner ordering, and $\lambda_i(\mathbf{B})$ is the i th largest eigenvalue. We let $\mathbf{1}_{\mathcal{E}}$ be the indicator function of an event \mathcal{E} , and $\neg\mathcal{E}$ for its complement event. We use $\text{Rate}(\mathbf{A}, k)$ as a short-hand for the sketch-and-project convergence rate (2) when $\mathbf{B} = \mathbf{I}$. We let C, C', C_1, c denote absolute constants whose values might differ from line to line.

Outline. The paper is organized as follows. In Section 2, we give formal statements and additional discussion of all our main results. In Section 3 we put them into perspective discussing some of the abundant related work on sketching and iterative sketching, as well as some prior approaches to the spectral analysis of $\mathbb{E}[\mathbf{P}]$. In Section 4, we give all the proofs, and supplement them with the empirical evidence in Section 5.

Acknowledgments. The authors are grateful to Michael Mahoney for valuable discussions regarding this paper.

2 Main results

In this section, we formulate our main theoretical results. Here and further, without loss of generality, we let $\mathbf{B} = \mathbf{I}$ in the formulation (1) of sketch-and-project (to revert this, it suffices to replace \mathbf{A} with $\mathbf{A}\mathbf{B}^{-1/2}$). The sketched projection matrix is then defined as:

$$\mathbf{P} := \mathbf{A}^\top \mathbf{S}^\top (\mathbf{S} \mathbf{A} \mathbf{A}^\top \mathbf{S}^\top)^\dagger \mathbf{S} \mathbf{A} = (\mathbf{S} \mathbf{A})^\dagger \mathbf{S} \mathbf{A},$$

where \mathbf{S} is $k \times m$. The iteration step of sketch-and-project reduces to the following update:

$$\mathbf{x}_{t+1} = \mathbf{x}_t - (\mathbf{S} \mathbf{A})^\dagger \mathbf{S} (\mathbf{A} \mathbf{x}_t - \mathbf{b}). \quad (6)$$

Relying on the characterization (5) given by [GR15], the convergence rate of the above update satisfies

$$\mathbb{E} \|\mathbf{x}_{t+1} - \mathbf{x}_*\|^2 \leq (1 - \lambda_{\min}(\mathbb{E}[\mathbf{P}])) \cdot \mathbb{E} \|\mathbf{x}_t - \mathbf{x}_*\|^2, \quad (7)$$

which means that $\text{Rate}(\mathbf{A}, k) \geq \lambda_{\min}(\mathbb{E}[\mathbf{P}])$, so in the remainder of this section we focus primarily on lower-bounding $\lambda_{\min}(\mathbb{E}[\mathbf{P}])$. Our bounds depend on the approximation quality of the subspace defined by the projection, as measured by the Frobenius error $\text{Err}(\mathbf{A}, k) = \mathbb{E} \|\mathbf{A}(\mathbf{I} - \mathbf{P})\|_F^2$ that arises in Randomized SVD.

2.1 Smallest eigenvalue analysis with Gaussian sketches

The first part of our results gives lower bounds for the spectrum of the sketched projection matrix in the case of standard Gaussian sketches. The result of Theorem 1 holds for any matrix $\mathbf{A} \in \mathbb{R}^{m \times n}$ and all sketch sizes up to $n/4 - o(n)$, see the details in Remark 1. It shows that the convergence rate improves at least linearly with respect to the sketch size k . Additionally, in Corollary 1, we show faster rate increases with respect to k for the matrices with fast spectral decays. The proofs for both Theorem 1 and Corollary 1 can be found in Section 4.1.

Theorem 1. *Let \mathbf{A} be an $m \times n$ matrix with rank n and let \mathbf{S} be a $k \times m$ Gaussian matrix. We denote the projection onto the span of $\mathbf{S} \mathbf{A}$, along with its Randomized SVD error, as:*

$$\mathbf{P} := (\mathbf{S} \mathbf{A})^\dagger \mathbf{S} \mathbf{A} \quad \text{and} \quad \text{Err}(\mathbf{A}, k) := \mathbb{E} \|\mathbf{A}(\mathbf{I} - \mathbf{P})\|_F^2. \quad (8)$$

Then, the smallest eigenvalue of $\mathbb{E}[\mathbf{P}]$ satisfies:

$$\lambda_{\min}(\mathbb{E}[\mathbf{P}]) \geq (1 - \epsilon) \frac{k \sigma_{\min}^2(\mathbf{A})}{\text{Err}(\mathbf{A}, k - 1)} \quad \text{where} \quad \epsilon \leq \frac{4k}{n} + \frac{8 \log(3n)}{n}. \quad (9)$$

Note that the right hand side uses $\text{Err}(\mathbf{A}, k - 1)$, i.e., Randomized SVD error based on a Gaussian matrix of size $k - 1$, even though the left hand side is defined using a sketch of size k . In particular, for $k = 1$ we get $\text{Err}(\mathbf{A}, 0)$, which simplifies to $\|\mathbf{A}\|_F^2$.

Remark 1 (Sketch size and dependence on ϵ). *For example, it can be verified that for any $n \geq 250$ and $k \leq n/5$ we have $\epsilon \leq 0.9$, whereas for any $n \geq 1000$ and $k \leq n/20$ we have $\epsilon \leq 0.25$ (see also Remark 4 for a version of Theorem 1 that applies to sketch sizes larger than $n/4$). If k is fixed and $n \rightarrow \infty$, then $\epsilon \rightarrow 0$. Thus, since $\text{Err}(\mathbf{A}, k-1) \leq \|\mathbf{A}\|_F^2$ for any $k \geq 1$, Theorem 1 immediately gives a simple guarantee for sketch-and-project:*

$$\text{Rate}(\mathbf{A}, k) \geq (1 - \epsilon_{n,k}) \frac{k\sigma_{\min}^2(\mathbf{A})}{\|\mathbf{A}\|_F^2} \xrightarrow{n \rightarrow \infty} \frac{k\sigma_{\min}^2(\mathbf{A})}{\|\mathbf{A}\|_F^2}. \quad (10)$$

When $k = 1$, this recovers the standard rate $\sigma_{\min}^2(\mathbf{A})/\|\mathbf{A}\|_F^2$ of Randomized Kaczmarz [SV09].

We note that even the simple bound (10) is often tighter than the earlier known bound for Gaussian Kaczmarz [RN21] (see (12) in Section 3.1), especially for larger sketch sizes. For matrices \mathbf{A} with known spectral decay, the main bound (15) gives room for tightening the estimate, as we see in the following corollary. This result combines our Theorem 1 with a bound on the Randomized SVD error given by [HMRT19] in the cases when \mathbf{A} exhibits polynomial or exponential spectral decays, which commonly arise in real-world data matrices. To highlight the improved dependence on sketch size k , we contrast this with the simple guarantee and let all rates scale with $\sigma_{\min}^2(\mathbf{A})/\|\mathbf{A}\|_F^2$.

Corollary 1. *Let \mathbf{A} be a full rank $m \times n$ matrix and let \mathbf{S} be a $k \times m$ Gaussian matrix. There is an absolute constant C such that for any $k = 1, \dots, n$, the sketch-and-project update (6) satisfies:*

$$\text{(general spectrum)} \quad \mathbb{E} \|\mathbf{x}_t - \mathbf{x}_*\|^2 \leq \left(1 - \frac{k\sigma_{\min}^2(\mathbf{A})}{C\|\mathbf{A}\|_F^2}\right)^t \cdot \|\mathbf{x}_0 - \mathbf{x}_*\|^2.$$

If we assume that \mathbf{A} has a polynomial spectral decay of order $\beta > 1$, i.e., $\sigma_i^2(\mathbf{A}) \leq ci^{-\beta}\sigma_1^2(\mathbf{A})$ for all i and some $c > 0$, then there is a constant $C = C(\beta, c)$ such that for any $k \leq n/2$:

$$\text{(polynomial decay)} \quad \mathbb{E} \|\mathbf{x}_t - \mathbf{x}_*\|^2 \leq \left(1 - \frac{k^\beta \sigma_{\min}^2(\mathbf{A})}{C\|\mathbf{A}\|_F^2}\right)^t \cdot \|\mathbf{x}_0 - \mathbf{x}_*\|^2.$$

If we assume that \mathbf{A} has an exponential spectral decay of order $\alpha > 1$, i.e., $\sigma_i^2(\mathbf{A}) \leq c\alpha^{-i}\sigma_1^2(\mathbf{A})$ for all i and some $c > 0$, then there is a constant $C = C(\alpha, c)$ such that for any $k \leq n/2$:

$$\text{(exponential decay)} \quad \mathbb{E} \|\mathbf{x}_t - \mathbf{x}_*\|^2 \leq \left(1 - \frac{\alpha^k \sigma_{\min}^2(\mathbf{A})}{C\|\mathbf{A}\|_F^2}\right)^t \cdot \|\mathbf{x}_0 - \mathbf{x}_*\|^2.$$

Finally, note that when the spectral distribution exhibits a sharp drop, implying that the Randomized SVD error rapidly shrinks at some k , the rate estimate from (9) will exhibit a similar rapid improvement for those sketch sizes. This suggests minimal viable sketch sizes that result in effective convergence rates for certain spectral profiles. See also Figures 1 and 4 for an empirical demonstration.

2.2 Full-spectrum analysis with sub-gaussian sketches

Dense Gaussian sketches present one of the most convenient models for analysis, but they are also the least practical. While it is often a perfect tool for observing the trends that are also exhibited by other sketching distributions, extending the results to more general sketching models is far from trivial. In this section, we present our second main result: a full-spectrum analysis of the expected sketched projection matrix for sketching distributions satisfying the following generic concentration assumptions.

Definition 1 (Sub-gaussian concentration). *A random variable X satisfies sub-gaussian concentration with constant K if $\inf \{t > 0 : \mathbb{E} \exp(X^2/t^2) \leq 2\} \leq K$. A random n -dimensional vector \mathbf{x} is K -sub-gaussian if $\mathbf{v}^\top \mathbf{x}$ satisfies sub-gaussian concentration with K for any unit vector \mathbf{v} .*

Definition 2 (Euclidean concentration). *A random n -dimensional vector \mathbf{x} satisfies Euclidean concentration with constant L if for any $m \times n$ matrix \mathbf{A} , the random variable $X = \|\mathbf{A}\mathbf{x}\| - \|\mathbf{A}\|_F$ is $L\|\mathbf{A}\|$ -sub-gaussian.*

These assumptions on the rows of the sketching matrix \mathbf{S} are designed so that they naturally capture the behavior of random vectors with i.i.d. sub-gaussian entries (including Gaussian vectors), but also, so that they can be later extended to sparse vectors. The proof of the following Theorem 2 can be found in Section 4.2.

Theorem 2. *Let \mathbf{A} be an $m \times n$ matrix with condition number $\kappa = \sigma_{\max}(\mathbf{A})/\sigma_{\min}(\mathbf{A})$ and stable rank $r = \|\mathbf{A}\|_F^2/\|\mathbf{A}\|^2$, and let \mathbf{S} be a $k \times m$ random matrix with i.i.d. isotropic K -sub-gaussian rows that satisfy Euclidean concentration with constant L . Let \mathbf{P} denote the projection onto the span of $\mathbf{S}\mathbf{A}$, and let $\text{Err}(\mathbf{A}, k)$ denote rank k Randomized SVD error, as per (8). There are absolute constants $C_1, C_2 > 0$ such that if $r \geq C_1 \max\{k, L^2 \log \kappa, K^4 L^2\}$, then:*

$$(1 - \epsilon)\bar{\mathbf{P}} \leq \mathbb{E}[\mathbf{P}] \leq (1 + \epsilon)\bar{\mathbf{P}},$$

$$\text{where } \bar{\mathbf{P}} = \gamma_k \mathbf{A}^\top \mathbf{A} (\gamma_k \mathbf{A}^\top \mathbf{A} + \mathbf{I})^{-1}, \quad \gamma_k = \frac{k}{\text{Err}(\mathbf{A}, k-1)}, \quad \text{and} \quad \epsilon \leq \frac{C_2 K^2 L}{\sqrt{r}}.$$

As a direct corollary, we obtain the following convergence guarantee for sketch-and-project.

Corollary 2. *Under the assumptions of Theorem 2, sketch-and-project using matrix \mathbf{S} satisfies:*

$$\text{Rate}(\mathbf{A}, k) \geq (1 - \epsilon) \frac{\gamma_k \sigma_{\min}^2(\mathbf{A})}{\gamma_k \sigma_{\min}^2(\mathbf{A}) + 1} \geq (1 - \epsilon) \left(1 - \frac{k}{n}\right) \frac{k \sigma_{\min}^2(\mathbf{A})}{\text{Err}(\mathbf{A}, k-1)}. \quad (11)$$

The intermediate expression, which comes directly from the formula for $\bar{\mathbf{P}}$, is potentially a sharper estimate of the convergence rate than the estimate derived in Theorem 1. The difference between the two estimates is absorbed by the factor $(1 - k/n)$, used to replace the denominator $\gamma_k \sigma_{\min}^2(\mathbf{A}) + 1$ with 1, and it is only substantial when k is close to n .

As a key motivation, consider matrix \mathbf{S}_k that consists of i.i.d. mean zero, unit variance and K -sub-gaussian entries (sub-gaussian sketch). Then, it satisfies the assumptions of Theorem 2 with constants K and $L = O(K^2)$ (e.g., see Section 4 of [Der22]). A practical example of this is the matrix of random ± 1 entries (Rademacher sketch) for which both K and L are small absolute constants, and so, the theorem holds for $r \geq O(k + \log \kappa)$ with $\epsilon = O(1/\sqrt{r})$. We note that the logarithmic dependence on the condition number κ is in general unavoidable due to rare adverse events that occur for discrete sketching distributions.

In addition to the more general sketching distribution, the main difference between Theorem 2 and Gaussian Theorem 1 is that it provides a full-spectrum analysis of the expected projection, i.e., it captures all its eigenvalues rather than just the smallest one. However, to achieve this, we must impose certain regularity assumptions on the data matrix \mathbf{A} . Namely, while Theorem 1 only assumed that \mathbf{A} has full column rank, here, we require the *stable* rank $r = \|\mathbf{A}\|_F^2/\|\mathbf{A}\|^2$ of \mathbf{A} to be sufficiently large (in particular, larger than the sketch size k). Roughly, this prevents a fast spectral decay in the top- k part of the spectrum of \mathbf{A} .

Remark 2 (Initial accelerated convergence of sketch-and-project). *While the rate of convergence of sketch-and-project methods is typically bounded by the smallest eigenvalue of the expected sketched projection matrix via (2), it is easy to see that all eigenvalues matter for the convergence. Specifically, written in eigenvector basis, the l -th component of the expected distance to the solution shrinks with the rate governed by the l -th eigenvalue of the expected projection matrix. Indeed, let $\mathbf{d}_t := \mathbf{x}_t - \mathbf{x}_*$. Then the iterate (6) can be equivalently rewritten as $\mathbf{d}_{t+1} = (\mathbf{I} - (\mathbf{S}\mathbf{A})^\dagger \mathbf{S}\mathbf{A})\mathbf{d}_t$ (essentially, the iterates \mathbf{d}_t solve the system $\mathbf{A}\mathbf{d} = \mathbf{0}$). Then,*

$$\mathbb{E}\langle \mathbf{d}_{t+1}, \mathbf{v}_l \rangle = \langle (\mathbf{I} - \mathbb{E}[\mathbf{P}])\mathbf{d}_t, \mathbf{v}_l \rangle = \langle \mathbf{d}_t, \mathbf{v}_l \rangle - \langle \mathbf{d}_t, \mathbb{E}[\mathbf{P}]\mathbf{v}_l \rangle = (1 - \lambda_l)\langle \mathbf{d}_t, \mathbf{v}_l \rangle,$$

where $(\lambda_l, \mathbf{v}_l)$ is an eigen-pair of $\mathbb{E}[\mathbf{P}]$. (Note that when \mathbf{S} is Gaussian, then the eigenvectors of $\mathbb{E}[\mathbf{P}]$ are the same as the right singular vectors of \mathbf{A} ; see Lemma 1.) As it was first noted for the Randomized Kaczmarz method in [Ste21], this implies faster convergence than the one guaranteed by (2), at least for the components of the error vector \mathbf{d}_t that are parallel to \mathbf{v}_l . At the same time, the components corresponding to leading singular vectors will shrink faster with the iteration process, eventually bringing the convergence rate to the regime given by (11).

Theorem 2 shows that the initial accelerated convergence rate of sketch-and-project has components of the size at least

$$\lambda_l \geq (1 - \epsilon) \frac{\gamma_k \sigma_l^2(\mathbf{A})}{\gamma_k \sigma_l^2(\mathbf{A}) + 1}, \quad \text{for } l = 1, \dots, n.$$

One can compare this to the initial speed up of Randomized Kaczmarz (where $k = 1$), given by $\lambda_l \geq \sigma_l^2(\mathbf{A}) / \|\mathbf{A}\|_F^2$ [Ste21]. Here, again, our result allows us to quantify the dependence of initial accelerated convergence on the sketch size k thanks to the term $\gamma_k = k / \text{Err}(\mathbf{A}, k - 1) \geq k / \|\mathbf{A}\|_F^2$.

The proof of Theorem 2 is inspired by techniques from asymptotic random matrix theory used to analyze Stieltjes transforms [SB95]. This approach yields $\bar{\mathbf{P}}$, which we call the *surrogate expression* for the expected projection matrix, since it can be viewed as an asymptotically exact formula if we let $m, n, r \rightarrow \infty$. As part of this analysis, we must control the concentration of random quadratic forms such as $\mathbf{s}_i^\top \mathbf{B} \mathbf{s}_i$, where \mathbf{s}_i^\top is a row of the sketching matrix \mathbf{S} and \mathbf{B} is some positive semidefinite matrix. For i.i.d. sub-gaussian sketches, such concentration can be ensured, e.g., by the classical Hanson-Wright inequality [RV13]. In our case, this is ensured by the more general condition of Euclidean concentration imposed on the rows of \mathbf{S} .

2.3 Extension to sparse sketches

In our next result, we show that our full-spectrum analysis of expected sketched projection applies not only to dense sub-gaussian sketches, but also to certain sparse sketching matrices. We rely on a sparse sketching technique called Leverage Score Sparsified (LESS) embeddings, which was recently introduced by [DLDM21] (the below definition is based on [Der22]). These sketches can be implemented much more efficiently, reducing the per-iteration cost of sketch-and-project, and can be viewed as a bridge between the fast but less stable block sketches and heavy but more stable Gaussian sketches.

Definition 3 (LESS embeddings [DLDM21, Der22]). *Consider a full rank $m \times n$ matrix \mathbf{A} and let $l_i = \mathbf{a}_i^\top (\mathbf{A}^\top \mathbf{A})^{-1} \mathbf{a}_i$ for $i = 1, \dots, m$ denote its leverage scores. Fixing absolute constants $C, K \geq 1$ and letting $\mathbf{e}_j \in \mathbb{R}^m$ be the j -th standard basis vector, we define a LESS embedding for \mathbf{A} with sketch size k and s non-zeros per row as a matrix \mathbf{S} with k i.i.d. row vectors given by:*

$$\frac{1}{\sqrt{k}} \sum_{i=1}^s \frac{r_i}{\sqrt{s p_{t_i}}} \mathbf{e}_{t_i}^\top,$$

where r_i are i.i.d. K -sub-gaussian random variables with mean zero and unit variance, and t_i are sampled i.i.d. from a probability distribution $p = (p_1, \dots, p_m)$ such that $p_i \geq l_i / (Cn)$ for all i .

We show that, when $m \gg n$, then a sparse LESS embedding sketch retains the same spectral properties of the expected sketched projection matrix as a dense sub-gaussian sketch as established in Theorem 2. The proof of the following Theorem 3 can be found below in Section 4.3.

Theorem 3. *Let \mathbf{A} be an $m \times n$ matrix with condition number $\kappa = \sigma_{\max}(\mathbf{A}) / \sigma_{\min}(\mathbf{A})$ and stable rank $r = \|\mathbf{A}\|_F^2 / \|\mathbf{A}\|^2$. Let \mathbf{P} denote the projection onto the span of $\mathbf{S}\mathbf{A}$, and let $\text{Err}(\mathbf{A}, k)$ denote rank k Randomized SVD error, as per (8). There are absolute constants $C_1, C_2, C_3 > 0$*

such that if \mathbf{S} is a LESS embedding of size k with $s \geq C_1 n \log(\kappa n)$ non-zeros per row, and if $r \geq C_2 \max\{k, \log \kappa\}$, then

$$(1 - \epsilon)\bar{\mathbf{P}} \leq \mathbb{E}[\mathbf{P}] \leq (1 + \epsilon)\bar{\mathbf{P}},$$

where $\bar{\mathbf{P}} = \gamma_k \mathbf{A}^\top \mathbf{A} (\gamma_k \mathbf{A}^\top \mathbf{A} + \mathbf{I})^{-1}$, $\gamma_k = \frac{k}{\text{Err}(\mathbf{A}, k - 1)}$, and $\epsilon \leq \frac{C_3}{\sqrt{r}}$.

Remark 3 (Generating LESS sketches). For a LESS embedding matrix \mathbf{S} of size k with s non-zero entries per row, computing the matrix product $\mathbf{S}\mathbf{A}$ costs $O(kns)$ operations. For $s = 1$, this is equivalent to computing a block sketch (that samples k rows of the matrix \mathbf{A}), whereas for $s = m$, it effectively corresponds to a dense sub-gaussian sketch, so LESS embeddings can be viewed as interpolating between those two extremes. To obtain a probability distribution $p = (p_1, \dots, p_m)$ satisfying the condition from Definition 3, we can use one of two preprocessing steps:

1. **Approximating leverage scores.** This can be done using standard techniques from RandNLA [DMIMW12, CW17] in time $O(\text{nnz}(\mathbf{A}) \log m + n^3 \log n)$, where $\text{nnz}(\mathbf{A})$ is the number of non-zeros in \mathbf{A} . This is less than the cost of solving the system when $m \gg n$. Then, we can define p using the obtained leverage score estimates.
2. **Randomized preconditioning.** Replacing \mathbf{A} and \mathbf{b} with $\tilde{\mathbf{A}} = \mathbf{H}\mathbf{D}\mathbf{A}$ and $\tilde{\mathbf{b}} = \mathbf{H}\mathbf{D}\mathbf{b}$, where \mathbf{H} is an $m \times m$ fast randomized Fourier/Hadamard transform and \mathbf{D} is diagonal with random ± 1 entries, does not change the solution \mathbf{x}_* , and with high probability, ensures that all the leverage scores of $\tilde{\mathbf{A}}$ are nearly uniform [Tro11, Lemma 3.3]. This operation costs $O(mn \log m)$ time and allows us to use a uniform distribution p . Similar preconditioning was proposed for Block Kaczmarz methods, e.g., in [NT14].

Note that in practice (and in our experimental section), it is typical to omit preconditioning and rely on the incoherence of many natural datasets.

We would also like to note that the dichotomy between block sketching (light and more dependent on the matrix structure) and dense sketching (slow and heavy, but more general and theoretically better understood) is notorious across the numerical methods involving sketching. For example, there are very simple convergence guarantees for Gaussian Sketched Motzkin method [RN19] and much more complex, depending on the dynamic range, rate estimates for Block Motzkin Method (SKM) [HM21]. The results we show here for LESS sketches are as succinct as for the dense case and theoretically allow for the sparsity s that is almost of the order of n non-zeros per m -dimensional row (where $m \gg n$ for a highly overdetermined linear system). Nevertheless, empirical results in Section 5 suggest that this sparsity level is still quite conservative, and our spectral analysis in practice applies to sketches where s is a small constant, which effectively replicates a block sketching procedure. It is also natural to ask whether our results can be extended to other popular sparse sketching operators, such as the CountSketch [CW17], or to other structured sketching operators such as subsampled randomized Hadamard/Fourier transforms [AC09]. We leave this as a direction for future work.

2.4 Extension to stochastic Newton methods

Our convergence analysis for sketch-and-project can be easily adapted to a number of randomized convex optimization algorithms from the literature [GKLR19, HDNR20, GMMN21, YLG22]. In this setting, the goal is to find $\mathbf{x}_* = \text{argmin}_{\mathbf{x}} f(\mathbf{x})$, for some convex function $f : \mathbb{R}^m \rightarrow \mathbb{R}$. Naturally, such a problem can be solved by repeatedly solving the Newton system, i.e., finding \mathbf{x}_{t+1} such that $\nabla^2 f(\mathbf{x}_t)(\mathbf{x}_{t+1} - \mathbf{x}_t) = \nabla f(\mathbf{x}_t)$ for $t = 0, 1, 2$, etc. To avoid the cost of solving the system exactly at each iteration, we can sketch it with a $k \times m$ random matrix \mathbf{S} .

For example, [GKLR19] proposed the following so-called Randomized Subspace Newton:

$$\mathbf{x}_{t+1} = \operatorname{argmin}_{\mathbf{x} \in \mathbb{R}^m} \|\mathbf{x} - \mathbf{x}_t\|_{\nabla^2 f(\mathbf{x}_t)}^2 \quad \text{such that} \quad \mathbf{S} \nabla^2 f(\mathbf{x}_t) (\mathbf{x} - \mathbf{x}_t) = \eta_t \cdot \mathbf{S} \nabla f(\mathbf{x}_t),$$

where η_t is an appropriately chosen step size. The expected convergence rate of this procedure is controlled by a quantity analogous to $\lambda_{\min}(\mathbb{E}[\mathbf{P}])$, except with the input matrix $\tilde{\mathbf{A}}$ replaced by the positive semidefinite square root of the Hessian matrix $\mathbf{H}_t = \nabla^2 f(\mathbf{x}_t)$, and the smallest eigenvalue λ_{\min} replaced by the smallest *positive* eigenvalue λ_{\min}^+ (thus, allowing the Hessian to be low-rank):

$$\mathbb{E}[f(\mathbf{x}_{t+1}) - f(\mathbf{x}_*)] \leq (1 - c\rho_t) \cdot \mathbb{E}[f(\mathbf{x}_t) - f(\mathbf{x}_*)] \quad \text{for } \rho_t = \lambda_{\min}^+(\mathbf{H}_t^{1/2} \mathbb{E}[\mathbf{S}^\top (\mathbf{S} \mathbf{H}_t \mathbf{S}^\top)^\dagger \mathbf{S}] \mathbf{H}_t^{1/2}),$$

where $c \in (0, 1)$ is a constant that depends on the smoothness and strong convexity of f . Also, [HDNR20] showed that, for a similar procedure with added cubic regularization, the convergence improves as we approach \mathbf{x}_* , so that $c \rightarrow 1$ and we can replace the changing Hessians \mathbf{H}_t in the definition of ρ_t with the fixed Hessian at the optimum, $\nabla^2 f(\mathbf{x}_*)$. Our guarantees from Theorems 1, 2, and 3 can be used to complete the above convergence characterization when \mathbf{S} is Gaussian, sub-gaussian or LESS, by lower bounding the ρ_t quantity, as summarized below.

Corollary 3. *Let \mathbf{H} be an $m \times m$ positive semidefinite matrix with rank n , and let \mathbf{S} be a $k \times m$ sketching matrix \mathbf{S} . Moreover, suppose that one of the following is true:*

1. \mathbf{S} is a Gaussian matrix and $\epsilon = \frac{4k}{n} + \frac{8 \log(3n)}{n}$;
2. \mathbf{S} is a sub-gaussian or LESS embedding matrix and $\epsilon = O(1/\sqrt{r} + k/n)$, where $r = \operatorname{tr}(\mathbf{H})/\|\mathbf{H}\|$ satisfies $r \geq C \max\{k, \log \kappa\}$, with $\kappa = \lambda_{\max}(\mathbf{H})/\lambda_{\min}^+(\mathbf{H})$.

Then, letting $\operatorname{Err}(\mathbf{A}, k)$ be the rank- k Randomized SVD error, as per (8), we have:

$$\lambda_{\min}^+(\mathbf{H}^{1/2} \mathbb{E}[\mathbf{S}^\top (\mathbf{S} \mathbf{H} \mathbf{S}^\top)^\dagger \mathbf{S}] \mathbf{H}^{1/2}) \geq (1 - \epsilon) \frac{k \lambda_{\min}^+(\mathbf{H})}{\operatorname{Err}(\mathbf{H}^{1/2}, k - 1)} \geq \frac{k \lambda_{\min}^+(\mathbf{H})}{\operatorname{tr}(\mathbf{H})}.$$

The proof of Corollary 3 is almost immediate. It follows from Theorems 1, 2 and 3 by setting $\mathbf{A} = \tilde{\mathbf{U}} \tilde{\mathbf{D}}^{1/2}$, where $\mathbf{K} = \mathbf{U} \mathbf{D} \mathbf{U}^\top$ is the eigendecomposition of \mathbf{H} , whereas $\tilde{\mathbf{U}} \in \mathbb{R}^{m \times n}$ and $\tilde{\mathbf{D}} \in \mathbb{R}^{n \times n}$ are truncated versions of \mathbf{U} and \mathbf{D} produced by omitting the parts corresponding to the 0 eigenvalue (if \mathbf{K} is not full-rank).

3 Background and related work

In this section, we put our results in perspective by discussing some relevant prior work. We start with different variants of the Kaczmarz algorithm for solving linear systems, and then discuss the extensions of sketch-and-project to various optimization tasks. Finally, we cover recent prior work on the spectral analysis of expected projection matrices.

3.1 Sketching for linear systems

One of the most popular variants of the sketch-and-project method is the Kaczmarz algorithm for solving linear systems [Kac37]. Starting from an arbitrary initial iterate, it solves the system $\mathbf{A} \mathbf{x} = \mathbf{b}$ by sequential projections onto its individual equations (rows of \mathbf{A} , denoted as \mathbf{a}_i^\top), namely,

$$\mathbf{x}_{t+1} = \mathbf{x}_t - \frac{\mathbf{a}_i^\top \mathbf{x}_t - b_i}{\|\mathbf{a}_i\|^2} \mathbf{a}_i.$$

This iterative scheme is especially efficient for solving tall highly overdetermined linear systems, or for the case when the equations of the system become available in the streaming way. Its convergence guarantees of the form (2) were first proved in [SV09] with $\operatorname{Rate}(\mathbf{A}, k) \geq \sigma_{\min}^2(\mathbf{A})/\|\mathbf{A}\|_F^2$

under a randomized sampling rule: index of the next equation i is chosen proportionally to the L_2 -norm of the row vector \mathbf{a}_i^\top . It is exactly equivalent to sketch-and-project update (2) with $\mathbf{B} = \mathbf{I}$ and $1 \times n$ sketching vectors sampled from a discrete distribution over the standard basis vectors in \mathbb{R}^n . In [GR17], the authors show that more efficient (but less convenient) sampling distributions exist for the same discrete set of 1-sparse samples.

Variants of the Kaczmarz method that exploit several rows at each iteration, often referred to as block methods, have been extensively studied. In [NT14], the authors show that faster expected convergence $\text{Rate}(\mathbf{A}, k) \geq c\sigma_{\min}^2(\mathbf{A})/\log(n)\|\mathbf{A}\|^2$ can be guaranteed for a particular block partition of the matrix \mathbf{A} . The same paper shows that, empirically, block Kaczmarz method significantly outperforms randomized Kaczmarz method. However, the extent of this advantage (depending both on the sketch size and on the structure of the matrix \mathbf{A}) remained somewhat mysterious. In the special case of sketch size $k = 2$, the rate acceleration was connected to the row coherence of the matrix \mathbf{A} [NW13]. Later, in [HM21], the rate of block Kaczmarz method was bounded by the rate of Sketched Kaczmarz-Motzkin method (SKM), that does not require a pre-determined block size or a fixed block partition. However, SKM iterations are less optimal than block Kaczmarz iterations, and its theoretical convergence rate depends on the dynamic range of the sampled sub-residual, a non-trivial quantity that implicitly depends on the spectral properties of the matrix \mathbf{A} .

In [RN21], the authors show a nearly-linear growth of the convergence rate with the sketch size, for continuous sketching distributions. Namely, it is proved that for some constant $C > 0$,

$$\text{Rate}(\mathbf{A}, k) \geq \frac{k\sigma_{\min}^2(\mathbf{A})}{C(\sqrt{k}\|\mathbf{A}\| + \|\mathbf{A}\|_F)^2}, \quad (12)$$

under the assumption that \mathbf{S} is a $k \times m$ matrix with independent standard Gaussian entries. Note that this establishes linear growth only for k that is smaller than the stable rank of the matrix \mathbf{A} . Compare this to our Corollary 1, where we show $\text{Rate}(\mathbf{A}, k) \geq ck\sigma_{\min}^2(\mathbf{A})/\|\mathbf{A}\|_F^2$ for arbitrary matrices, and even better rates under certain spectral decay assumptions. Although the analysis in [RN21] can be slightly extended towards more general sketching distributions, one of the key parts of the proof is a random matrix deviation inequality resulting in the unavoidable mixture of the spectral and Frobenius norm in the denominator. In this work, we propose a new approach for the analysis of the random sketched projection matrix, based on rank one update formulas rather than on splitting a matrix into a product of two matrices followed by decoupling.

3.2 Sketch-and-project beyond linear systems

We treated linear solvers as our main application example mainly because it is a useful showcase of the phenomena appearing in sketch-and-project methods, related to the sketch sizes and sketching distributions, as well as the spectral properties of the data matrix. However, our analysis is applicable to any instance of sketch-and-project. A direct extension of solving overdetermined linear systems is feasibility questions for linear and convex feasibility problems, studied in the sketch-and-project viewpoint in [NT21]. Special cases of projection-based algorithms for linear feasibility, as well as their block variants, were studied earlier in [Agm54, LL10, BN15, DLHN17].

Further, numerous extensions of sketch-and-project have been aimed at efficiently minimizing convex functions [GKLR19, HDNR20], solving nonlinear equations [YLG22] and inverting matrices [GR17]. In Section 2.4, we explain how our convergence results can be extended to these settings using the example of minimizing convex functions with stochastic Newton methods [GKLR19, HDNR20]. This is possible whenever the convergence analysis relies on the smallest eigenvalue of the expected sketched projection matrix, sometimes referred to as the *stochastic condition number* in this line of works. Other examples where this setup occurs include the Sketched Newton-Raphson algorithm [YLG22] and the Stochastic Iterative Matrix Inversion algorithm [GR17].

3.3 Spectral analysis of expected projections

Full-spectrum analysis of the expected projection is generally not available for most block sampling distributions (i.e., those that select a random subset of rows of \mathbf{A}).

One notable exception is sketches based on Determinantal Point Processes (DPPs, [DM21]). These are distributions over subsets of rows, where not only the individual row probabilities, but also their pairwise correlations, are carefully chosen based on the matrix \mathbf{A} . The resulting sketch is therefore more expensive to construct, although practical algorithms are available in some settings [Der19, CDV20]. In this context, [MDK20] and [RK20] gave exact characterizations of the spectrum of $\mathbb{E}[\mathbf{P}]$ under certain DPP distributions, and they used these characterizations to analyze the convergence of a coordinate descent method based on sketch-and-project. These results were later extended and adapted to Randomized SVD-type error bounds [DKM20] and interpolated regression analysis [DLM20]. This line of works relies on proof techniques which are unique to DPP-based sketches, and therefore it is much less broadly applicable, compared to our unified analysis of Gaussian, sub-gaussian and sparse sketching matrices.

In the context of sub-gaussian sketches, full-spectrum analysis of the expected projection matrix was initiated by [DLLM20]. Their primary focus is on Randomized SVD, rather than sketch-and-project, and so, they study the full-spectrum analysis of the expected *residual* projection, i.e., $\mathbb{E}[\mathbf{I} - \mathbf{P}]$, rather than $\mathbb{E}[\mathbf{P}]$. This difference is crucial in the context of sketch-and-project, where the goal is to lower-bound the smallest eigenvalue of $\mathbb{E}[\mathbf{P}]$. Clearly, we have $\lambda_{\min}(\mathbb{E}[\mathbf{P}]) = 1 - \lambda_{\max}(\mathbb{E}[\mathbf{I} - \mathbf{P}])$, so a multiplicative upper bound on the largest eigenvalue of the residual projection, i.e., $\lambda_{\max}(\mathbb{E}[\mathbf{I} - \mathbf{P}]) \leq (1 + \epsilon) \cdot (1 - \rho)$ implies a much weaker *additive* bound on the convergence rate, i.e., $\lambda_{\min}(\mathbb{E}[\mathbf{P}]) \geq \rho - \epsilon$. Such a bound follows from Theorem 1 in [DLLM20], and gives

$$\text{Rate}(\mathbf{A}, k) \geq \rho - \epsilon \quad \text{with} \quad \rho = \frac{\gamma_k \sigma_{\min}^2(\mathbf{A})}{\gamma_k \sigma_{\min}^2(\mathbf{A}) + 1} \quad \text{and} \quad \epsilon = O\left(\frac{1}{\sqrt{r}}\right),$$

where r is the stable rank of the data matrix and γ_k is as in Theorem 2. For this bound to be non-vacuous, we must have $\epsilon < \rho$. Since ρ scales with the smallest singular value of \mathbf{A} , this means that the worst-case convergence rate bound derived from their result is completely vacuous unless the condition number of \mathbf{A} is close to 1. In this work, we perform the full-spectrum analysis directly on the expected projection, rather than its residual, and as a result, are able to obtain a *multiplicative* bound on the smallest eigenvalue, i.e., $\lambda_{\min}(\mathbb{E}[\mathbf{P}]) \geq (1 - \epsilon) \cdot \rho$, which is non-vacuous as long as $\epsilon < 1$, regardless of the value of ρ . To achieve this, in our analysis (proof of Theorem 2 in Section 4.2) we must overcome a key obstacle that does not arise in [DLLM20]: the rank-one decomposition of the expected projection matrix yields potentially non-symmetric and highly ill-conditioned random matrices. We address this by a careful symmetrization argument (steps 3 and 4), combined with a self-recursive bound (step 5).

4 Proofs of theoretical results

In this section, we give proofs for all the results formulated in Section 2.

4.1 Gaussian sketching: proof of Theorem 1

We start with several auxiliary results. The first one uses the rotational invariance of Gaussian distribution allowing us to pick a convenient basis for the sketched projection matrix. It follows by an argument similar to the one used in [CF11, Section 3.1].

Lemma 1. *Let \mathbf{A} be an $m \times n$ matrix with rank n , and $\mathbf{A} = \mathbf{U}\mathbf{D}\mathbf{V}^\top$ its compact singular value decomposition. Let \mathbf{S} and \mathbf{Z} be $k \times m$ and $k \times n$ Gaussian matrices, with $\mathbf{P} = (\mathbf{S}\mathbf{A})^\dagger \mathbf{S}\mathbf{A}$ and $\tilde{\mathbf{P}} = (\mathbf{Z}\mathbf{D})^\dagger \mathbf{Z}\mathbf{D}$. Then:*

1. The matrices $\mathbb{E}[\mathbf{P}]$ and $\mathbb{E}[\tilde{\mathbf{P}}]$ share the same spectrum.
2. The matrices $\mathbb{E}[\tilde{\mathbf{P}}]$ and \mathbf{D} share the same (standard) eigenbasis.
3. The Gaussian Randomized SVD error (8) satisfies $\text{Err}(\mathbf{A}, k) = \text{Err}(\mathbf{D}, k)$.

Proof. We start with the following preliminary consideration: note that a matrix function $\mathbf{M} : \text{Sym}(n) \rightarrow \text{Sym}(n)$ defined as

$$\mathbf{M}(\boldsymbol{\Sigma}) := \mathbb{E}[\boldsymbol{\Sigma}^{1/2} \mathbf{Z}^\top (\mathbf{Z} \boldsymbol{\Sigma} \mathbf{Z}^\top)^\dagger \mathbf{Z} \boldsymbol{\Sigma}^{1/2}]$$

is an *isotropic tensor function*, i.e., that $\mathbf{M}(\mathbf{Q} \boldsymbol{\Sigma} \mathbf{Q}^\top) = \mathbf{Q} \mathbf{M}(\boldsymbol{\Sigma}) \mathbf{Q}^\top$ for all $n \times n$ orthogonal matrices \mathbf{Q} . This follows because, due to rotational invariance of the Gaussian distribution, random matrix $\mathbf{Z} \mathbf{Q}$ is distributed identically as \mathbf{Z} for any orthogonal \mathbf{Q} , so we have for any symmetric positive semidefinite matrix $\boldsymbol{\Sigma}$:

$$\begin{aligned} \mathbf{M}(\mathbf{Q} \boldsymbol{\Sigma} \mathbf{Q}^\top) &= \mathbb{E}[\mathbf{Q} \boldsymbol{\Sigma}^{1/2} \mathbf{Q}^\top \mathbf{Z}^\top (\mathbf{Z} \mathbf{Q} \boldsymbol{\Sigma} \mathbf{Q}^\top \mathbf{Z}^\top)^\dagger \mathbf{Z} \mathbf{Q} \boldsymbol{\Sigma}^{1/2} \mathbf{Q}^\top] \\ &= \mathbf{Q} \mathbb{E}[\boldsymbol{\Sigma}^{1/2} (\mathbf{Z} \mathbf{Q})^\top (\mathbf{Z} \mathbf{Q} \boldsymbol{\Sigma} (\mathbf{Z} \mathbf{Q})^\top)^\dagger \mathbf{Z} \mathbf{Q} \boldsymbol{\Sigma}^{1/2}] \mathbf{Q}^\top = \mathbf{Q} \mathbf{M}(\boldsymbol{\Sigma}) \mathbf{Q}^\top. \end{aligned}$$

Additionally, from the literature on continuum mechanics (see Section 6.4 in [Its07]; e.g., Theorem 6.2), it is known that any isotropic tensor function $\mathbf{M}(\boldsymbol{\Sigma})$ has the same eigenbasis as $\boldsymbol{\Sigma}$. Equipped with that, we are ready to prove the three claims of the lemma:

1. Note that

$$\mathbb{E}[\mathbf{P}] = \mathbb{E}[(\mathbf{Z} \mathbf{D} \mathbf{V}^\top)^\dagger \mathbf{Z} \mathbf{D} \mathbf{V}^\top] = \mathbf{M}(\mathbf{V} \mathbf{D}^2 \mathbf{V}^\top) = \mathbf{V} \mathbf{M}(\mathbf{D}^2) \mathbf{V}^\top = \mathbf{V} \mathbb{E}[\tilde{\mathbf{P}}] \mathbf{V}^\top, \quad (13)$$

since the matrices $\mathbf{S} \mathbf{U}$ and \mathbf{Z} are equidistributed due to rotational invariance of the Gaussian distribution, and then we use the isotropic tensor property of \mathbf{M} . The claim follows since spectrum is preserved under orthogonal rotations.

2. The matrix \mathbf{D} has the same (standard) basis as \mathbf{D}^2 , which is the same as the basis of $\mathbf{M}(\mathbf{D}^2)$ due to the isotropic tensor property.
3. Due to circular trace property, linearity of expectation and (13), we can rewrite

$$\begin{aligned} \text{Err}(\mathbf{A}, k) &= \text{tr}(\mathbf{A}^\top \mathbf{A} (\mathbf{I} - \mathbb{E}[\mathbf{P}])) = \text{tr}(\mathbf{V} \mathbf{D}^2 \mathbf{V}^\top (\mathbf{I} - \mathbf{M}(\mathbf{V} \mathbf{D}^2 \mathbf{V}^\top))) \\ &= \text{tr}(\mathbf{V} \mathbf{D}^2 \mathbf{V}^\top (\mathbf{I} - \mathbf{V} \mathbf{M}(\mathbf{D}^2) \mathbf{V}^\top)) \\ &= \text{tr}(\mathbf{D}^2 (\mathbf{I} - \mathbf{M}(\mathbf{D}^2))) = \text{Err}(\mathbf{D}, k). \end{aligned}$$

This concludes the proof of Lemma 1. □

The next two lemmas recall standard linear algebra and high-dimensional probability tools. We include them in the convenient formulations for completeness of the argument. The first lemma is a well-known Sherman-Morrison rank one update formula.

Lemma 2 (Sherman-Morrison formula). *For an invertible matrix $\mathbf{A} \in \mathbb{R}^{n \times n}$ and $\mathbf{u}, \mathbf{v} \in \mathbb{R}^n$, $\mathbf{A} + \mathbf{u} \mathbf{v}^\top$ is invertible if and only if $1 + \mathbf{v}^\top \mathbf{A}^{-1} \mathbf{u} \neq 0$. If this holds, then*

$$(\mathbf{A} + \mathbf{u} \mathbf{v}^\top)^{-1} = \mathbf{A}^{-1} - \frac{\mathbf{A}^{-1} \mathbf{u} \mathbf{v}^\top \mathbf{A}^{-1}}{1 + \mathbf{v}^\top \mathbf{A}^{-1} \mathbf{u}}.$$

In particular, it follows that:

$$(\mathbf{A} + \mathbf{u} \mathbf{v}^\top)^{-1} \mathbf{u} = \frac{\mathbf{A}^{-1} \mathbf{u}}{1 + \mathbf{v}^\top \mathbf{A}^{-1} \mathbf{u}}.$$

The next lemma is essentially a sharper version of the Hanson-Wright concentration inequality for Gaussian vectors.

Lemma 3. *For any fixed $n \times n$ positive semidefinite matrix \mathbf{Y} , an n -dimensional standard Gaussian vector \mathbf{s} , and any $\alpha > 0$, let*

$$\mathcal{E}_\alpha := \{\mathbf{s}^\top \mathbf{Y} \mathbf{s} \leq \text{tr } \mathbf{Y} + \sqrt{2\alpha \text{tr}(\mathbf{Y}^2)} + \alpha \|\mathbf{Y}\|\}.$$

Then

$$\mathbb{P}[-\mathcal{E}_\alpha] \leq \exp(-\alpha/2) \quad \text{and} \quad \mathbb{E}[\mathbf{s}^\top \mathbf{Y} \mathbf{s} \cdot \mathbf{1}_{-\mathcal{E}_\alpha}] \leq 5 \text{tr}(\mathbf{Y}) \cdot e^{-\alpha/2}. \quad (14)$$

Proof. The first claim of (14) is a sharper version of Hanson-Wright inequality for Gaussian vectors, proved in [HKZ⁺12]. So, $\mathbb{E}[\mathbf{1}_{-\mathcal{E}_\alpha}] = \mathbb{P}(-\mathcal{E}_\alpha) \leq e^{-\alpha/2}$. Letting $u_\alpha := \sqrt{2\alpha \text{tr}(\mathbf{Y}^2)} + \alpha \|\mathbf{Y}\|$, we have for the second claim:

$$\begin{aligned} \mathbb{E}[(\mathbf{s}^\top \mathbf{Y} \mathbf{s}) \mathbf{1}_{-\mathcal{E}_\alpha}] &\leq \text{tr } \mathbf{Y} \cdot e^{-\alpha/2} + \mathbb{E}[(\mathbf{s}^\top \mathbf{Y} \mathbf{s} - \text{tr } \mathbf{Y}) \mathbf{1}_{-\mathcal{E}_\alpha}] \\ &= \text{tr } \mathbf{Y} \cdot e^{-\alpha/2} + \int_{u_\alpha}^{\infty} \mathbb{P}[\mathbf{s}^\top \mathbf{Y} \mathbf{s} \geq \text{tr } \mathbf{Y} + t] dt \\ &\leq \text{tr } \mathbf{Y} \cdot e^{-\alpha/2} + \int_{u_\alpha}^{\infty} \exp\left(-\min\left\{\frac{t^2}{4 \text{tr}(\mathbf{Y}^2)}, \frac{t}{2\|\mathbf{Y}\|}\right\}\right) dt \\ &\leq \text{tr } \mathbf{Y} \cdot e^{-\alpha/2} + \sqrt{4 \text{tr}(\mathbf{Y}^2)} \cdot e^{-\alpha/2} + 2\|\mathbf{Y}\| \cdot e^{-\alpha/2} \\ &\leq 5 \text{tr } \mathbf{Y} \cdot e^{-\alpha/2}. \end{aligned}$$

This concludes the proof of the lemma. □

The last auxiliary result is our key proposition that connects a form of the expected sketched matrix with the standard Randomized SVD error (compare with (3)):

Proposition 1. *Let \mathbf{A} be an $m \times n$ matrix, \mathbf{S} be a $k \times m$ Gaussian matrix, and $\mathbf{P} = (\mathbf{S}\mathbf{A})^\dagger \mathbf{S}\mathbf{A}$. Then, for any event \mathcal{E} such that the rows of $\mathbf{S}\mathbf{A}$ are identically distributed conditioned on \mathcal{E} , we have*

$$\mathbb{E}[\text{tr}(\mathbf{S}\mathbf{A}\mathbf{A}^\top \mathbf{S}^\top)^{-1} \mid \mathcal{E}] \geq \frac{k \mathbb{P}(\mathcal{E})}{\text{Err}(\mathbf{A}, k-1)},$$

where $\text{Err}(\mathbf{A}, k) := \mathbb{E} \|\mathbf{A}(\mathbf{I} - \mathbf{P})\|_F^2$.

Proof. Let $\mathbf{x}_i \in \mathbb{R}^n$ be the i -th row of a random matrix $\mathbf{X} := \mathbf{S}\mathbf{A} \in \mathbb{R}^{k \times n}$. By a standard Schur complement result (e.g., [BV04]) applied to a block decomposition of the matrix $(\mathbf{S}\mathbf{A}\mathbf{A}^\top \mathbf{S}^\top)^{-1} = (\mathbf{X}\mathbf{X}^\top)^{-1} \in \mathbb{R}^{k \times k}$ separating an (i, i) -th entry into a 1×1 block, we have for any $i = 1, \dots, k$,

$$\begin{aligned} [(\mathbf{X}\mathbf{X}^\top)^{-1}]_{ii} &= (\|\mathbf{x}_i\|^2 - \mathbf{x}_i^\top \mathbf{X}_{-i}^\top (\mathbf{X}_{-i} \mathbf{X}_{-i}^\top)^{-1} \mathbf{X}_{-i} \mathbf{x}_i)^{-1} \\ &= (\|\mathbf{x}_i\|^2 - \mathbf{x}_i^\top \mathbf{X}_{-i}^\dagger \mathbf{X}_{-i} \mathbf{x}_i)^{-1} = \frac{1}{\mathbf{x}_i^\top \mathbf{P}_{\perp i} \mathbf{x}_i}, \end{aligned}$$

where $\mathbf{X}_{-i} \in \mathbb{R}^{(k-1) \times n}$ is the matrix obtained by deleting the i -th row from \mathbf{X} , $\mathbf{P}_{-i} = (\mathbf{X}_{-i})^\dagger \mathbf{X}_{-i}$, and $\mathbf{P}_{\perp i} := \mathbf{I} - \mathbf{P}_{-i}$. Since for all i both \mathbf{x}_i and $\mathbf{P}_{\perp i}$ have the same distribution conditioned on the event \mathcal{E} , we can conclude that

$$\mathbb{E}[\text{tr}(\mathbf{X}\mathbf{X}^\top)^{-1} \mid \mathcal{E}] = \sum_{i=1}^k \mathbb{E}[(\mathbf{X}\mathbf{X}^\top)^{-1} \mid \mathcal{E}]_{ii} = \mathbb{E}\left[\frac{k}{\mathbf{x}_k^\top \mathbf{P}_{\perp k} \mathbf{x}_k} \mid \mathcal{E}\right].$$

Now, using Jensen's inequality,

$$\mathbb{E} \left[\frac{k}{\mathbf{x}_k^\top \mathbf{P}_{\perp k} \mathbf{x}_k} \mid \mathcal{E} \right] \geq \frac{k}{\mathbb{E}[\mathbf{x}_k^\top \mathbf{P}_{\perp k} \mathbf{x}_k \mid \mathcal{E}]} \geq \frac{k\mathbb{P}(\mathcal{E})}{\mathbb{E}[\mathbf{x}_k^\top \mathbf{P}_{\perp k} \mathbf{x}_k]}$$

and the claim is concluded as follows:

$$\begin{aligned} \mathbb{E}[\mathbf{x}_k^\top \mathbf{P}_{\perp k} \mathbf{x}_k] &= \mathbb{E}[\mathbb{E}_{\mathbf{x}_k}(\mathbf{x}_k^\top \mathbf{P}_{\perp k} \mathbf{x}_k \mid \mathbf{P}_{\perp k})] \\ &= \mathbb{E}[\text{tr}(\mathbf{A} \mathbf{P}_{\perp k} \mathbf{A}^\top)] \\ &= \mathbb{E}[\text{tr}(\mathbf{A} \mathbf{P}_{\perp k} \mathbf{P}_{\perp k}^\top \mathbf{A}^\top)] = \mathbb{E}\|\mathbf{A} \mathbf{P}_{\perp k}\|_F^2. \end{aligned}$$

Since $\mathbf{A} \mathbf{P}_{\perp k} = \mathbf{A}(\mathbf{I} - \mathbf{P}^{(k-1)})$ for a $k-1 \times m$ standard Gaussian matrix $\mathbf{P}^{(k-1)}$, this concludes the proof of Proposition 1. \square

Proof of Theorem 1. First, rotational invariance of the standard Gaussian matrix \mathbf{S} allows us to pass to a very convenient basis, as shown in Lemma 1. Therefore, with a slight abuse of notation, we will assume that \mathbf{S} is a $k \times n$ Gaussian matrix, $\mathbf{A} = \mathbf{D}$ is an $n \times n$ diagonal matrix and $\sigma_1 \geq \sigma_2 \geq \dots \geq \sigma_n > 0$ are its diagonal entries (and eigenvalues), $\mathbf{P} = (\mathbf{S}\mathbf{D})^\dagger(\mathbf{S}\mathbf{D})$. Let $\{\mathbf{e}_1, \dots, \mathbf{e}_n\}$ be the standard Euclidean eigenbasis of both $\mathbb{E}[\mathbf{P}]$ and \mathbf{D} . By Lemma 1, we will conclude the statement of the theorem by showing that

$$\lambda_{\min}(\mathbb{E}[\mathbf{P}]) = \min_i \mathbb{E}[\mathbf{e}_i^\top \mathbf{P} \mathbf{e}_i] \geq (1 - \epsilon) \frac{k\lambda_{\min}^2(\mathbf{D})}{\text{Err}(\mathbf{D}, k-1)}. \quad (15)$$

We will do this in several steps.

Step 1. Sherman-Morrison lemma and Gaussian quadratic forms. By the definition of pseudoinverse,

$$\mathbf{e}_i^\top \mathbf{P} \mathbf{e}_i = \mathbf{e}_i^\top \mathbf{D} \mathbf{S}^\top (\mathbf{S} \mathbf{D}^2 \mathbf{S}^\top)^{-1} \mathbf{S} \mathbf{D} \mathbf{e}_i = \sigma_i^2 \hat{\mathbf{s}}_i^\top (\mathbf{S} \mathbf{D}^2 \mathbf{S}^\top)^{-1} \hat{\mathbf{s}}_i = \sigma_i^2 \hat{\mathbf{s}}_i^\top \mathbf{Y} \hat{\mathbf{s}}_i,$$

where $\hat{\mathbf{s}}_i$ denotes the i -th column vector of \mathbf{S} , and $\mathbf{Y} := (\mathbf{S} \mathbf{D}^2 \mathbf{S}^\top)^{-1}$. Then, by a version of Sherman-Morrison rank one update formula (Lemma 2),

$$\mathbf{e}_i^\top \mathbf{P} \mathbf{e}_i = \sigma_i^2 \hat{\mathbf{s}}_i^\top (\mathbf{S} \mathbf{D}_{-i}^2 \mathbf{S}^\top + \sigma_i^2 \hat{\mathbf{s}}_i \hat{\mathbf{s}}_i^\top)^{-1} \hat{\mathbf{s}}_i = \frac{\sigma_i^2 \hat{\mathbf{s}}_i^\top (\mathbf{S} \mathbf{D}_{-i}^2 \mathbf{S}^\top)^{-1} \hat{\mathbf{s}}_i}{1 + \sigma_i^2 \hat{\mathbf{s}}_i^\top (\mathbf{S} \mathbf{D}_{-i}^2 \mathbf{S}^\top)^{-1} \hat{\mathbf{s}}_i},$$

where \mathbf{D}_{-i}^2 denote \mathbf{D}^2 with i th diagonal entry zeroed out. Then, since $\mathbf{S} \mathbf{D}_{-i}^2 \mathbf{S}^\top$ is independent from $\hat{\mathbf{s}}_i$, and $\mathbf{S} \mathbf{D}_{-i}^2 \mathbf{S}^\top \leq \mathbf{S} \mathbf{D}^2 \mathbf{S}^\top = \mathbf{Y}^{-1}$, we get:

$$\min_i \mathbb{E}[\mathbf{e}_i^\top \mathbf{P} \mathbf{e}_i] \geq \min_i \mathbb{E} \left[\frac{\sigma_i^2 \mathbf{s}^\top \mathbf{Y} \mathbf{s}}{1 + \sigma_i^2 \mathbf{s}^\top \mathbf{Y} \mathbf{s}} \right] = \mathbb{E} \left[\frac{\sigma_n^2 \mathbf{s}^\top \mathbf{Y} \mathbf{s}}{1 + \sigma_n^2 \mathbf{s}^\top \mathbf{Y} \mathbf{s}} \right], \quad (16)$$

where \mathbf{s} is a new k -dimensional Gaussian vector independent of \mathbf{S} (and so, of \mathbf{Y}), and we used that a function $f(\sigma) = \sigma^2 x / (1 + \sigma^2 x)$ is increasing for all $x > 0$.

Step 2. Gaussian Hanson-Wright inequality and removing dependence on \mathbf{s} . Note that $\mathbb{E} \mathbf{s}^\top \mathbf{Y} \mathbf{s} = \text{tr}(\mathbf{Y})$. For any $\alpha > 0$, the event

$$\mathcal{E}_\alpha := \{\mathbf{s}^\top \mathbf{Y} \mathbf{s} \leq w_\alpha(\mathbf{Y})\} \quad \text{with} \quad w_\alpha(\mathbf{Y}) := \text{tr} \mathbf{Y} + \sqrt{2\alpha \text{tr}(\mathbf{Y}^2)} + \alpha \|\mathbf{Y}\|$$

has $\mathbb{P}(\mathcal{E}_\alpha | \mathbf{Y}) \geq 1 - e^{-\alpha/2}$ and $\mathbb{E}[\mathbf{s}^\top \mathbf{Y} \mathbf{s} \cdot \mathbf{1}_{-\mathcal{E}_\alpha} | \mathbf{Y}] \leq 5 \text{tr}(\mathbf{Y}) \cdot e^{-\alpha/2}$ by a sharper Gaussian version of Hanson-Wright formula (Lemma 3). This implies

$$\begin{aligned} \mathbb{E}_\mathbf{s} \left[\frac{\sigma_n^2 \mathbf{s}^\top \mathbf{Y} \mathbf{s}}{1 + \sigma_n^2 \mathbf{s}^\top \mathbf{Y} \mathbf{s}} \mid \mathbf{Y} \right] &\geq \mathbb{E}_\mathbf{s} \left[\frac{\mathbf{s}^\top \mathbf{Y} \mathbf{s}}{\sigma_n^{-2} + \mathbf{s}^\top \mathbf{Y} \mathbf{s}} \cdot \mathbf{1}_{\mathcal{E}_\alpha} \mid \mathbf{Y} \right] \\ &\geq \frac{\text{tr} \mathbf{Y} - \mathbb{E}[\mathbf{s}^\top \mathbf{Y} \mathbf{s} \cdot \mathbf{1}_{-\mathcal{E}_\alpha} | \mathbf{Y}]}{\sigma_n^{-2} + w_\alpha(\mathbf{Y})} \geq (1 - 5e^{-\alpha/2}) \frac{\text{tr} \mathbf{Y}}{\sigma_n^{-2} + w_\alpha(\mathbf{Y})}. \end{aligned}$$

Further, let $\mathcal{U}_\alpha := \{w_\alpha(\mathbf{Y}) \leq t_\alpha\}$ for some t_α to be defined later. Note that:

$$\mathbb{E}_{\mathbf{Y}} \left[\frac{\text{tr } \mathbf{Y}}{\sigma_n^{-2} + w_\alpha(\mathbf{Y})} \right] \geq \mathbb{P}(\mathcal{U}_\alpha) \mathbb{E} \left[\frac{\text{tr } \mathbf{Y}}{\sigma_n^{-2} + w_\alpha(\mathbf{Y})} \mid \mathcal{U}_\alpha \right] \geq \mathbb{P}(\mathcal{U}_\alpha) \frac{\mathbb{E}[\text{tr } \mathbf{Y} \mid \mathcal{U}_\alpha]}{\sigma_n^{-2} + t_\alpha}$$

So, by (16) and independence of \mathbf{Y} and \mathbf{s} ,

$$\min_i \mathbb{E}[\mathbf{e}_i^\top \mathbf{P} \mathbf{e}_i] = \min_i \mathbb{E}_{\mathbf{Y}} (\mathbb{E}_{\mathbf{s}}[\mathbf{e}_i^\top \mathbf{P} \mathbf{e}_i \mid \mathbf{Y}]) \geq (1 - 5e^{-\alpha/2}) \mathbb{P}(\mathcal{U}_\alpha) \frac{\mathbb{E}[\text{tr } \mathbf{Y} \mid \mathcal{U}_\alpha]}{\sigma_n^{-2} + t_\alpha}. \quad (17)$$

Step 3. Using Proposition 1 and final probability estimates. Note that both trace and spectral norm of \mathbf{Y} are invariant with respect to the permutations of the rows of $\mathbf{S}\boldsymbol{\Sigma}^{1/2}$, so conditioning on the event \mathcal{U}_α keeps the rows identically distributed and we can apply Proposition 1 to estimate the leftover expectation term. As a result, we have that

$$\mathbb{E}[\text{tr } \mathbf{Y} \mid \mathcal{U}_\alpha] \geq \frac{k \mathbb{P}(\mathcal{U}_\alpha)}{\text{Err}(\mathbf{D}, k-1)}$$

and

$$\min_i \mathbb{E}[\mathbf{e}_i^\top \mathbf{P} \mathbf{e}_i] \geq \frac{(1 - 5e^{-\alpha/2}) \mathbb{P}^2(\mathcal{U}_\alpha)}{1 + t_\alpha \sigma_n^2} \cdot \frac{k \lambda_{\min}^2(\mathbf{D})}{\text{Err}(\mathbf{D}, k-1)}. \quad (18)$$

To conclude the desired lower bound (15), we only need to choose t_α to make $\mathbb{P}(\mathcal{U}_\alpha)$ sufficiently large so that

$$\frac{(1 - 5e^{-\alpha/2}) \mathbb{P}^2(\mathcal{U}_\alpha)}{1 + t_\alpha \sigma_n^2} \geq 1 - \epsilon. \quad (19)$$

Recall that $\mathbf{Y} = (\mathbf{S}\mathbf{D}^2\mathbf{S}^\top)^{-1}$ and $\mathcal{U}_\alpha = \{\text{tr } \mathbf{Y} + \sqrt{2\alpha \text{tr } \mathbf{Y}^2} + \alpha \|\mathbf{Y}\| \leq t_\alpha\}$. A direct computation connects all three terms to the spectral properties of the Gaussian $k \times n$ sketch matrix \mathbf{S} as follows:

- $\text{tr } \mathbf{Y} \leq \sigma_n^{-2} \cdot \text{tr}(\mathbf{S}\mathbf{S}^\top)^{-1} \leq k\sigma_n^{-2} \cdot \|(\mathbf{S}\mathbf{S}^\top)^{-1}\|$,
- $\sqrt{\text{tr } \mathbf{Y}^2} \leq \sqrt{k}\sigma_n^{-2} \cdot \|(\mathbf{S}\mathbf{S}^\top)^{-1}\|$,
- $\|\mathbf{Y}\| \leq \sigma_n^{-2} \cdot \|(\mathbf{S}\mathbf{S}^\top)^{-1}\|$.

The spectral norm of the inverse $\|(\mathbf{S}\mathbf{S}^\top)^{-1}\| = \sigma_{\max}^2(\mathbf{S}^{-1}) = \sigma_{\min}^{-2}(\mathbf{S})$ can be bounded by the following sharp concentration inequality for standard Gaussian matrices (e.g., [DS01]):

$$\mathbb{P}[\sigma_{\min}^2(\mathbf{S}) \leq (\sqrt{n} - \sqrt{k} - \sqrt{\alpha})^2] \leq \exp(-\alpha/2).$$

It implies that $\mathbb{P}(\mathcal{U}_\alpha) \geq 1 - e^{-\alpha/2}$ if we choose

$$t_\alpha := \frac{\sigma_n^{-2} \cdot (k + \sqrt{2\alpha k} + \alpha)}{(\sqrt{n} - \sqrt{k} - \sqrt{\alpha})^2} \leq \sigma_n^{-2} \cdot \left(\frac{\sqrt{k} + \sqrt{\alpha}}{\sqrt{n} - \sqrt{k} - \sqrt{\alpha}} \right)^2.$$

Thus, with $\rho = \left(\frac{\sqrt{k} + \sqrt{\alpha}}{\sqrt{n}} \right)^2$, $\delta = 7e^{-\alpha/2}$ and $\alpha = 2 \log n$, we have:

$$\begin{aligned} \epsilon &= 1 - \frac{(1 - 5e^{-\alpha/2}) \mathbb{P}^2(\mathcal{U}_\alpha)}{1 + t_\alpha \sigma_n^2} \leq 1 - \frac{1 - 7e^{-\alpha/2}}{1 + \left(\frac{\sqrt{k} + \sqrt{\alpha}}{\sqrt{n} - \sqrt{k} - \sqrt{\alpha}} \right)^2} \\ &= \frac{1}{\left(\frac{1}{\sqrt{\rho}} - 1 \right)^2 + 1} + \frac{\delta}{1 + \frac{1}{\left(\frac{1}{\sqrt{\rho}} - 1 \right)^2}} \leq 2\rho + \delta \\ &= \frac{2(\sqrt{k} + \sqrt{2 \log n})^2 + 7}{n} \leq \frac{4k}{n} + \frac{8 \log(3n)}{n}, \end{aligned}$$

where we used the fact that for any $x > 0$ we have:

$$\frac{1}{\left(\frac{1}{\sqrt{x}} - 1\right)^2 + 1} = \frac{2x}{1 + (1 - 2\sqrt{x})^2} \leq 2x.$$

This concludes (19) with $\epsilon \leq \frac{4k}{n} + \frac{8\log(3n)}{n}$ and thus Theorem 1 follows from (18) and (15). \square

Remark 4. By setting $\alpha = 4$ above, one can also obtain the following bound for $k < (\sqrt{n} - 2)^2$:

$$\lambda_{\min}(\mathbb{E}[\mathbf{P}]) \geq \frac{0.05}{1 + C} \cdot \frac{k\sigma_{\min}^2(\mathbf{A})}{\text{Err}(\mathbf{A}, k - 1)} \quad \text{where} \quad C = \left(\frac{\sqrt{k} + 2}{\sqrt{n} - \sqrt{k} - 2}\right)^2.$$

This bound is less sharp than Theorem 1 for small sketch sizes k , but it is non-vacuous for a wider range of values of n and k . In particular, we have $C \leq 10$ when $n \geq 100$ and $k \leq n/2$.

Next, we are going to give a proof for Corollary 1. It relies on the following known spectral estimate for Randomized SVD with Gaussian sketching.

Lemma 4 ([HMT11], Theorem 10.5). *Let \mathbf{A} be an $m \times n$ matrix, \mathbf{S} be a $k \times m$ Gaussian matrix with $k \geq 2$, and $\mathbf{P} = (\mathbf{S}\mathbf{A})^\dagger \mathbf{S}\mathbf{A}$. For any $2 \leq p \leq k - 2$, Randomized SVD error $\text{Err}(\mathbf{A}, k) = \mathbb{E} \|\mathbf{A}(\mathbf{I} - \mathbf{P})\|_F^2$ satisfies:*

$$\text{Err}(\mathbf{A}, k) \leq \frac{k-1}{p-1} \cdot \sum_{i \geq k-p} \sigma_i^2,$$

where $\sigma_1 \geq \sigma_2 \geq \dots$ are the singular values of \mathbf{A} .

Proof of Corollary 1. Without loss of generality, assume that $n \geq 100$. For convenience, we will use the bound from Remark 4, and combine this with (7). The first claim follows immediately from Remark 4 for sketch sizes $k \leq n/2$, since $\text{Err}(\mathbf{A}, k) \leq \|\mathbf{A}\|_F^2$. To show it for larger sizes, it suffices to observe that $\lambda_{\min}(\mathbb{E}[\mathbf{P}])$ is non-decreasing as a function of k , so if we show a lower bound for $k = n/2$, then the same bound holds for $k > n/2$. The factor 2 in the bound (coming from using a different k) can be absorbed into the constant.

We next prove the polynomial decay part of Corollary 1, by combining Remark 4 with Lemma 4. Without loss of generality, assume that $k \geq 4\beta$ and set $p = k/\beta - 1$ in the lemma. We can now bound the Randomized SVD error for sketch size $k - 1$:

$$\begin{aligned} \text{Err}(\mathbf{A}, k - 1) &\leq \frac{k-2}{p-1} \cdot \sum_{i \geq k-1-p} \sigma_i^2 \leq \frac{k-2}{\frac{k}{\beta} - 2} \cdot c\sigma_1^2 \sum_{i \geq k-1-p} i^{-\beta} \\ &\leq \beta \frac{k-2}{k-2\beta} \cdot \frac{c\sigma_1^2}{(\beta-1)(k-1-p)^{\beta-1}} \\ &\leq \frac{k-2}{k-2\beta} \cdot \left(\frac{\beta}{\beta-1}\right)^\beta \frac{c\sigma_1^2}{k^{\beta-1}} \leq \frac{k-2}{k-2\beta} \cdot \frac{\beta}{\beta-1} \cdot \frac{ec\sigma_1^2}{k^{\beta-1}}. \end{aligned}$$

As a result, using Theorem 1 (Remark 4) and letting $\kappa(\mathbf{A}) = \sigma_{\max}(\mathbf{A})/\sigma_{\min}(\mathbf{A})$, we conclude that there is a constant $C > 0$ such that:

$$\lambda_{\min}(\mathbb{E}[\mathbf{P}]) \geq \left(1 - 2\frac{\beta-1}{k-2}\right) \left(1 - \frac{1}{\beta}\right) \cdot \frac{k^\beta}{Cck^2(\mathbf{A})}.$$

So, since $\kappa^2(\mathbf{A}) \geq \|\mathbf{A}\|_F^2/\sigma_{\min}^2(\mathbf{A})$ and $k \geq 4\beta$, we get the claim by adjusting the constant. The result for exponential decay follows analogously, using Lemma 4 with $p = 2$. \square

4.2 Sub-gaussian sketching: proof of Theorem 2

Let us first set up some notations to be used throughout this section.

Let $\mathbf{x}_i \in \mathbb{R}^n$ be the i -th row of \mathbf{SA} , i.e., $\mathbf{x}_i = \mathbf{A}^\top \mathbf{s}_i$ for $\mathbf{s}_i \in \mathbb{R}^m$ the i -th row of \mathbf{S} . Let us denote a ‘‘truncated’’ projection with one row less by $\mathbf{P}_{-i} = (\mathbf{S}_{-i} \mathbf{A})^\dagger \mathbf{S}_{-i} \mathbf{A}$ for $\mathbf{S}_{-i} \in \mathbb{R}^{(k-1) \times n}$ the matrix obtained by deleting the i -th row from \mathbf{S} . We will also frequently refer to the residual projections and denote them by $\mathbf{P}_\perp = \mathbf{I} - \mathbf{P}$, $\bar{\mathbf{P}}_\perp := \mathbf{I} - \bar{\mathbf{P}}$, and $\mathbf{P}_{\perp i} := \mathbf{I} - \mathbf{P}_{-i}$. Recall that $\mathbf{P} = (\mathbf{SA})^\dagger \mathbf{SA}$ and its surrogate $\bar{\mathbf{P}} := \gamma \boldsymbol{\Sigma} (\gamma \boldsymbol{\Sigma} + \mathbf{I})^{-1}$, where $\boldsymbol{\Sigma} = \mathbf{A}^\top \mathbf{A}$ and $\gamma = \gamma_k := k/\mathbb{E} \|\mathbf{AP}_{\perp k}\|_F^2$. Let $\sigma_1^2 \geq \sigma_2^2 \geq \dots \geq \sigma_n^2$ be the eigenvalues of $\boldsymbol{\Sigma}$.

Lemma 5. *Let \mathbf{A} be an $m \times n$ matrix with stable rank $r = \|\mathbf{A}\|_F^2 / \|\mathbf{A}\|^2$, and let \mathbf{S} be a $k \times m$ random matrix with i.i.d. rows that satisfy L -Euclidean concentration (Definition 2). In the notations outlined above, consider the events*

$$\mathcal{E}_i := \left\{ \mathbf{x}_i^\top \mathbf{P}_{\perp i} \mathbf{x}_i \geq \frac{1}{2} \text{tr} \boldsymbol{\Sigma} \mathbf{P}_{\perp i} \right\}, \quad \text{and} \quad \mathcal{E} := \bigwedge_{i=1}^k \mathcal{E}_i. \quad (20)$$

Then

$$\delta := \mathbb{P}(-\mathcal{E}) \leq 2 \exp(-cr/L^2). \quad (21)$$

Proof. Due to L -Euclidean concentration of each row of the sketching matrix \mathbf{S} and independence between \mathbf{x}_i and \mathbf{P}_{-i} ,

$$\mathbb{P}(-\mathcal{E}_i) \leq \mathbb{E} 2 \exp \left(-c \frac{\text{tr} \boldsymbol{\Sigma} \mathbf{P}_{\perp i}}{L^2 \|\mathbf{AP}_{\perp i}\|^2} \right) \leq 2 \exp(-c(r-k)/L^2),$$

where we conditioned on a realization of the matrix \mathbf{P}_{-i} , and then use the fact that

$$\text{tr} \boldsymbol{\Sigma} \mathbf{P}_{\perp i} \geq \sum_{i \geq k} \sigma_i^2 \geq \sum_i \sigma_i^2 - \sigma_1^2 k \geq \sigma_1^2 (r-k) \geq \|\mathbf{AP}_{\perp i}\|^2 (r-k).$$

Finally, $\mathbb{P}(-\mathcal{E}) \leq 2k \exp(-c(r-k)/L^2) \leq 2 \exp(-c'r/L^2)$. \square

A key technical step of the proof of Theorem 2 is the following convenient split of the symmetric spectral difference between expected sketched matrix and its surrogate into three parts (this initial splitting is similar – but not identical – with the first step in [DLLM20]):

Lemma 6. *Let \mathbf{A} be a full rank $m \times n$ matrix and let \mathbf{S} be a $k \times m$ random sketching matrix with i.i.d. rows having mean zero and identity covariance. Then, in the notations outlined above in the beginning of Section 4.2, for any positive probability event \mathcal{E} ,*

$$\begin{aligned} \|\bar{\mathbf{P}}^{-1/2} \mathbb{E}_{\mathcal{E}}[\mathbf{P}] \bar{\mathbf{P}}^{-1/2} - \mathbf{I}\| &\leq \left\| \boldsymbol{\Sigma}^{-1/2} \mathbb{E}_{\mathcal{E}}[\mathbf{P}_{\perp k} \mathbf{x}_k \mathbf{x}_k^\top - \mathbf{P}_{\perp k} \boldsymbol{\Sigma}] \boldsymbol{\Sigma}^{-1/2} \right\| + \left\| \boldsymbol{\Sigma}^{-1/2} \mathbb{E}_{\mathcal{E}}[\mathbf{P}_{\perp k} \boldsymbol{\Sigma} - \mathbf{P}_{\perp k} \boldsymbol{\Sigma}] \boldsymbol{\Sigma}^{-1/2} \right\| \\ &+ \left\| \mathbb{E}_{\mathcal{E}} \left[\left(\frac{\mathbb{E}[\mathbf{x}_k^\top \mathbf{P}_{\perp k} \mathbf{x}_k]}{\mathbf{x}_k^\top \mathbf{P}_{\perp k} \mathbf{x}_k} - 1 \right) \cdot \boldsymbol{\Sigma}^{-1/2} \mathbf{P}_{\perp k} \mathbf{x}_k \mathbf{x}_k^\top \boldsymbol{\Sigma}^{-1/2} \right] \right\|. \end{aligned}$$

The proof of Lemma 6 relies on another version of a rank one update formula, which proof can be found in [Mey73, DLLM20].

Lemma 7 ([Mey73, DLLM20]). *For $\mathbf{X} \in \mathbb{R}^{k \times n}$ with $k < n$, denote $\mathbf{P} = \mathbf{X}^\dagger \mathbf{X}$ and $\mathbf{P}_{-k} = \mathbf{X}_{-k}^\dagger \mathbf{X}_{-k}$, with $\mathbf{X}_{-i} \in \mathbb{R}^{(k-1) \times n}$ the matrix \mathbf{X} without its i -th row $\mathbf{x}_i \in \mathbb{R}^n$. Then, as long as $\mathbf{x}_k^\top (\mathbf{I} - \mathbf{P}_{-k}) \mathbf{x}_k \neq 0$, we have:*

$$(\mathbf{X}^\top \mathbf{X})^\dagger \mathbf{x}_k = \frac{(\mathbf{I} - \mathbf{P}_{-k}) \mathbf{x}_k}{\mathbf{x}_k^\top (\mathbf{I} - \mathbf{P}_{-k}) \mathbf{x}_k}, \quad \mathbf{P} - \mathbf{P}_{-k} = \frac{(\mathbf{I} - \mathbf{P}_{-k}) \mathbf{x}_k \mathbf{x}_k^\top (\mathbf{I} - \mathbf{P}_{-k})}{\mathbf{x}_k^\top (\mathbf{I} - \mathbf{P}_{-k}) \mathbf{x}_k}.$$

Proof of Lemma 6. Since for $\mathbf{X} = \mathbf{S}\mathbf{A}$,

$$\mathbb{E}\mathbf{P} = \mathbb{E}(\mathbf{X}^\dagger \mathbf{X}) = \mathbb{E}(\mathbf{X}^T \mathbf{X})^\dagger (\mathbf{X}^T \mathbf{X}) = \sum_{i=1}^k \mathbb{E}(\mathbf{X}^T \mathbf{X})^\dagger \mathbf{x}_i \mathbf{x}_i^T = k \mathbb{E}(\mathbf{X}^T \mathbf{X})^\dagger \mathbf{x}_k \mathbf{x}_k^T,$$

we have by Lemma 7 below

$$\mathbb{E}\mathbf{P} = k \mathbb{E} \left[\frac{(\mathbf{I} - \mathbf{P}_{-k}) \mathbf{x}_k \mathbf{x}_k^T}{\mathbf{x}_k^T (\mathbf{I} - \mathbf{P}_{-k}) \mathbf{x}_k} \right]. \quad (22)$$

One can check directly that $\bar{\mathbf{P}}^{-1} = (\boldsymbol{\Sigma} + \gamma^{-1} \mathbf{I}) \boldsymbol{\Sigma}^{-1}$. Therefore, also using that $\|\mathbf{U}\mathbf{V}\| \leq \|\mathbf{V}\mathbf{U}\|$ if $\mathbf{U}\mathbf{V}$ is symmetric (see also the discussion near (24) below),

$$\begin{aligned} \|\bar{\mathbf{P}}^{-1/2} \mathbb{E}_{\mathcal{E}}[\mathbf{P}] \bar{\mathbf{P}}^{-1/2} - \mathbf{I}\| &= \|\bar{\mathbf{P}}^{-1/2} [\mathbb{E}_{\mathcal{E}}[\mathbf{P}] \bar{\mathbf{P}}^{-1} - \mathbf{I}] \bar{\mathbf{P}}^{1/2}\| \\ &= \|(\boldsymbol{\Sigma} + \gamma^{-1} \mathbf{I})^{1/2} \boldsymbol{\Sigma}^{-1/2} (\mathbb{E}_{\mathcal{E}}[\mathbf{P}] \gamma^{-1} \boldsymbol{\Sigma}^{-1} - \mathbb{E}_{\mathcal{E}}[\mathbf{P}_{\perp}]) \boldsymbol{\Sigma}^{1/2} (\boldsymbol{\Sigma} + \gamma^{-1} \mathbf{I})^{-1/2}\| \\ &\leq \|\boldsymbol{\Sigma}^{-1/2} \mathbb{E}_{\mathcal{E}}[\mathbf{P}] \gamma^{-1} \boldsymbol{\Sigma}^{-1/2} - \boldsymbol{\Sigma}^{-1/2} \mathbb{E}_{\mathcal{E}}[\mathbf{P}_{\perp}] \boldsymbol{\Sigma}^{1/2}\| \\ &\stackrel{(22)}{=} \left\| \gamma^{-1} \boldsymbol{\Sigma}^{-1/2} \mathbb{E}_{\mathcal{E}} \left[\frac{k \mathbf{P}_{\perp k} \mathbf{x}_k \mathbf{x}_k^T}{\mathbf{x}_k^T \mathbf{P}_{\perp k} \mathbf{x}_k} \right] \boldsymbol{\Sigma}^{-1/2} - \boldsymbol{\Sigma}^{-1/2} \mathbb{E}_{\mathcal{E}}[\mathbf{P}_{\perp} \boldsymbol{\Sigma}] \boldsymbol{\Sigma}^{-1/2} \right\|. \end{aligned}$$

Now, note that by definition of γ , we have $k/\gamma = \mathbb{E}\|\mathbf{A}\mathbf{P}_{\perp k}\|_F^2 = \mathbb{E}\text{tr}(\boldsymbol{\Sigma}\mathbf{P}_{\perp k}) = \mathbb{E}[\mathbf{x}_k^T \mathbf{P}_{\perp k} \mathbf{x}_k]$ and we can continue with $\xi := \mathbf{x}_k^T \mathbf{P}_{\perp k} \mathbf{x}_k$

$$\begin{aligned} \|\bar{\mathbf{P}}^{-1/2} \mathbb{E}_{\mathcal{E}}[\mathbf{P}] \bar{\mathbf{P}}^{-1/2} - \mathbf{I}\| &\leq \left\| \mathbb{E}_{\mathcal{E}} \left[\frac{\mathbb{E}\xi}{\xi} \cdot \boldsymbol{\Sigma}^{-1/2} \mathbf{P}_{\perp k} \mathbf{x}_k \mathbf{x}_k^T \boldsymbol{\Sigma}^{-1/2} \right] - \boldsymbol{\Sigma}^{-1/2} \mathbb{E}_{\mathcal{E}}[\mathbf{P}_{\perp} \boldsymbol{\Sigma}] \boldsymbol{\Sigma}^{-1/2} \right\| \\ &\leq \left\| \mathbb{E}_{\mathcal{E}} \left[\left(\frac{\mathbb{E}\xi}{\xi} - 1 \right) \cdot \boldsymbol{\Sigma}^{-1/2} \mathbf{P}_{\perp k} \mathbf{x}_k \mathbf{x}_k^T \boldsymbol{\Sigma}^{-1/2} \right] \right\| \\ &\quad + \left\| \boldsymbol{\Sigma}^{-1/2} \mathbb{E}_{\mathcal{E}}[\mathbf{P}_{\perp k} \mathbf{x}_k \mathbf{x}_k^T - \mathbf{P}_{\perp k} \boldsymbol{\Sigma}] \boldsymbol{\Sigma}^{-1/2} \right\| \\ &\quad + \left\| \boldsymbol{\Sigma}^{-1/2} \mathbb{E}_{\mathcal{E}}[\mathbf{P}_{\perp k} \boldsymbol{\Sigma} - \mathbf{P}_{\perp} \boldsymbol{\Sigma}] \boldsymbol{\Sigma}^{-1/2} \right\|. \end{aligned}$$

□

The last technical lemma quantifies the variance of the quadratic forms with the vectors under Euclidean concentration:

Lemma 8. *Let \mathbf{x} be an n -dimensional isotropic random vector that satisfies Euclidean concentration with constant L . Then, for any $n \times n$ matrix \mathbf{B} , we have:*

$$\text{Var}[\mathbf{x}^T \mathbf{B} \mathbf{x}] \leq CL^2 \|\mathbf{B}\| (L^2 \|\mathbf{B}\| + \|\mathbf{B}\|_*).$$

Proof. First, suppose that $\mathbf{B} = \mathbf{A}^T \mathbf{A}$ for some matrix \mathbf{A} . Note that from Euclidean concentration we have that $\mathbb{E}[(\|\mathbf{A}\mathbf{x}\| - \|\mathbf{A}\|_F)^p] \leq CL^p \|\mathbf{A}\|^p$ for $p = 2, 4$. Thus, we have

$$\begin{aligned} \text{Var}[\mathbf{x}^T \mathbf{B} \mathbf{x}] &= \mathbb{E}[(\|\mathbf{A}\mathbf{x}\|^2 - \|\mathbf{A}\|_F^2)^2] \\ &= \mathbb{E}[(\|\mathbf{A}\mathbf{x}\| - \|\mathbf{A}\|_F)^2 (\|\mathbf{A}\mathbf{x}\| + \|\mathbf{A}\|_F)^2] \\ &\leq 2 \mathbb{E}[(\|\mathbf{A}\mathbf{x}\| - \|\mathbf{A}\|_F)^4] + 8 \|\mathbf{A}\|_F^2 \mathbb{E}[(\|\mathbf{A}\mathbf{x}\| - \|\mathbf{A}\|_F)^2] \\ &\leq 2CL^4 \|\mathbf{A}\|^4 + 8 \|\mathbf{A}\|_F^2 CL^2 \|\mathbf{A}\|^2 \\ &= 2CL^2 \|\mathbf{B}\| (L^2 \|\mathbf{B}\| + 4\|\mathbf{B}\|_*), \end{aligned}$$

Adjusting the constants we obtain the claim for a symmetric positive semidefinite \mathbf{B} . Next, suppose that \mathbf{B} is only symmetric. Then, we can decompose it as a difference of two positive semidefinite matrices: $\mathbf{B} = \mathbf{B}_+ - \mathbf{B}_-$, and moreover we have:

$$\begin{aligned}\text{Var}[\mathbf{x}^\top \mathbf{B} \mathbf{x}] &= \mathbb{E} \left[\left(\mathbf{x}^\top \mathbf{B}_+ \mathbf{x} - \text{tr}(\mathbf{B}_+) - (\mathbf{x}^\top \mathbf{B}_- \mathbf{x} - \text{tr}(\mathbf{B}_-)) \right)^2 \right] \\ &\leq 2\text{Var}[\mathbf{x}^\top \mathbf{B}_+ \mathbf{x}] + 2\text{Var}[\mathbf{x}^\top \mathbf{B}_- \mathbf{x}] \\ &\leq 2CL^2 \|\mathbf{B}_+\| (L^2 \|\mathbf{B}_+\| + \|\mathbf{B}_+\|_*) + 2CL^2 \|\mathbf{B}_-\| (L^2 \|\mathbf{B}_-\| + \|\mathbf{B}_-\|_*) \\ &\leq 4CL^2 \|\mathbf{B}\| (L^2 \|\mathbf{B}\| + \|\mathbf{B}\|_*).\end{aligned}$$

Finally, for a general matrix \mathbf{B} , it suffices to observe that $\mathbf{x}^\top \mathbf{B} \mathbf{x} = \mathbf{x}^\top \bar{\mathbf{B}} \mathbf{x}$ for a symmetric matrix $\bar{\mathbf{B}} = (\mathbf{B} + \mathbf{B}^\top)/2$, which completes the proof. \square

Now, we are ready to proceed with the proof of Theorem 2.

Proof of Theorem 2. Without loss of generality (rescaling both \mathbf{A} and γ), we will assume that

$$\|\boldsymbol{\Sigma}\| = 1 \quad \Rightarrow \quad \|\boldsymbol{\Sigma}^{-1/2}\| = \kappa; \quad \text{tr}(\boldsymbol{\Sigma}) = r. \quad (23)$$

1. Symmetrization, initial conditioning and the three part splitting. We are going to use throughout the proof a simple fact that for any two square matrices \mathbf{X} and \mathbf{Y} , if $\mathbf{X}\mathbf{Y}$ is symmetric (while $\mathbf{Y}\mathbf{X}$ may not be), then:

$$\|\mathbf{X}\mathbf{Y}\| = \rho(\mathbf{X}\mathbf{Y}) = \rho(\mathbf{Y}\mathbf{X}) \leq \|\mathbf{Y}\mathbf{X}\|, \quad (24)$$

where we use $\rho(\mathbf{B}) = \max_i \{|\lambda_i(\mathbf{B})|\}$ to denote the spectral radius of \mathbf{B} . This is the reason we will try to keep the expressions we work with symmetric. In particular, the claim of Theorem 2 is equivalent to proving that

$$\rho := \|\bar{\mathbf{P}}^{-1/2} \mathbb{E}[\mathbf{P}] \bar{\mathbf{P}}^{-1/2} - \mathbf{I}\| \leq CLK^2 / \sqrt{r} \quad (25)$$

for some universal constant $C > 0$. Now, let us pass to a version of (25) conditioned on the event \mathcal{E} defined as in (20). Here and further, $\mathbb{E}_{\mathcal{E}}$ denotes corresponding conditional expectation.

$$\begin{aligned}\|\bar{\mathbf{P}}^{-1/2} \mathbb{E}[\mathbf{P}] \bar{\mathbf{P}}^{-1/2} - \mathbf{I}\| &\leq \|\bar{\mathbf{P}}^{-1/2} \mathbb{E}_{\mathcal{E}}[\mathbf{P}] \bar{\mathbf{P}}^{-1/2} - \mathbf{I}\| + \|\bar{\mathbf{P}}^{-1/2} (\mathbb{E}_{\mathcal{E}}[\mathbf{P}] - \mathbb{E}[\mathbf{P}]) \bar{\mathbf{P}}^{-1/2}\| \\ &\leq \|\bar{\mathbf{P}}^{-1/2} \mathbb{E}_{\mathcal{E}}[\mathbf{P}] \bar{\mathbf{P}}^{-1/2} - \mathbf{I}\| + \|\bar{\mathbf{P}}^{-1}\| \cdot \|\mathbb{E}_{\mathcal{E}}[\mathbf{P}] - \mathbb{E}[\mathbf{P}]\| \cdot \mathbb{P}(-\mathcal{E}) \\ &\leq \|\bar{\mathbf{P}}^{-1/2} \mathbb{E}_{\mathcal{E}}[\mathbf{P}] \bar{\mathbf{P}}^{-1/2} - \mathbf{I}\| + \|\bar{\mathbf{P}}^{-1}\| \cdot 2 \cdot \delta,\end{aligned}$$

where $\delta = \exp(-cr/L^2)$ by Lemma 5. We also have $\|\bar{\mathbf{P}}^{-1}\| = \|\mathbf{I} + \gamma^{-1} \boldsymbol{\Sigma}^{-1}\| \leq 1 + \kappa^2/\gamma \leq 1 + r\kappa^2$ since $r = \text{tr}(\boldsymbol{\Sigma}) \geq \mathbb{E}\|\mathbf{A}\mathbf{P}_{\perp k}\|_F^2$. So,

$$\rho \leq \rho_{\mathcal{E}} + 2(1 + r\kappa^2)\delta, \quad \text{where} \quad \rho_{\mathcal{E}} := \|\bar{\mathbf{P}}^{-1/2} \mathbb{E}_{\mathcal{E}}[\mathbf{P}] \bar{\mathbf{P}}^{-1/2} - \mathbf{I}\|. \quad (26)$$

Now, since by Theorem 2 assumption $r \geq CL^2 \log \kappa$ for sufficiently large constant $C > 0$, then $\delta r \kappa^2 \leq \exp(2 \log \kappa + \log r - cr/L^2) \leq \exp(-c'r/L^2)$. So, instead of (25), it is enough to prove that $\rho_{\mathcal{E}} \leq CLK^2 / \sqrt{r}$. The first bound on $\rho_{\mathcal{E}}$ is given by Lemma 6:

$$\begin{aligned}\rho_{\mathcal{E}} &\leq T_1 + T_2 + T_3, \\ \text{where } T_1 &:= \left\| \boldsymbol{\Sigma}^{-1/2} \mathbb{E}_{\mathcal{E}}[\mathbf{P}_{\perp k} \mathbf{x}_k \mathbf{x}_k^\top - \mathbf{P}_{\perp k} \boldsymbol{\Sigma}] \boldsymbol{\Sigma}^{-1/2} \right\|, \\ T_2 &:= \left\| \boldsymbol{\Sigma}^{-1/2} \mathbb{E}_{\mathcal{E}}[\mathbf{P}_{\perp k} \boldsymbol{\Sigma} - \mathbf{P}_{\perp k} \boldsymbol{\Sigma}] \boldsymbol{\Sigma}^{-1/2} \right\|, \\ T_3 &:= \left\| \mathbb{E}_{\mathcal{E}} \left[\frac{\mathbb{E}[\xi] - \xi}{\xi} \cdot \boldsymbol{\Sigma}^{-1/2} \mathbf{P}_{\perp k} \mathbf{x}_k \mathbf{x}_k^\top \boldsymbol{\Sigma}^{-1/2} \right] \right\|,\end{aligned}$$

with $\xi := \mathbf{x}_k^\top \mathbf{P}_{\perp k} \mathbf{x}_k$ and $\mathbb{E}[\xi] = \mathbb{E}\text{tr}(\boldsymbol{\Sigma} \mathbf{P}_{\perp k}) = \mathbb{E}\|\mathbf{A} \mathbf{P}_{\perp k}\|_F^2 = k/\gamma$.

2. Bounding T_1 . First, note that the conditioning is the only reason for T_1 to be non-zero. Indeed, since the rows of \mathbf{S} are isotropic and $\mathbf{x}_k = \mathbf{A}^\top \mathbf{s}_k$, letting $\Xi := \mathbf{P}_{\perp k}(\mathbf{x}_k \mathbf{x}_k^\top - \boldsymbol{\Sigma})$, we have:

$$\mathbb{E}[\Xi] = \mathbb{E}[\mathbf{P}_{\perp k} \mathbb{E}[\mathbf{x}_k \mathbf{x}_k^\top - \boldsymbol{\Sigma} \mid \mathbf{P}_{\perp k}]] = \mathbf{0}.$$

By the law of total probability, this also implies that

$$\mathbb{E}_{\mathcal{E}}[\Xi] = -\mathbb{E}[\mathbf{1}_{-\mathcal{E}} \Xi] / \mathbb{P}(\mathcal{E}) \leq \frac{\mathbb{E}[\mathbf{1}_{-\mathcal{E}} \Xi]}{1 - \delta}.$$

Now, using $\|\mathbf{P}_{\perp k}\| = 1$ as a projection matrix, we have

$$\begin{aligned} T_1 &\leq \kappa^2 \|\mathbb{E}_{\mathcal{E}}[\mathbf{P}_{\perp k}(\mathbf{x}_k \mathbf{x}_k^\top - \boldsymbol{\Sigma})]\| \leq \frac{\kappa^2}{1 - \delta} \|\mathbb{E}[\mathbf{1}_{-\mathcal{E}} \mathbf{P}_{\perp k}(\mathbf{x}_k \mathbf{x}_k^\top - \boldsymbol{\Sigma})]\| \\ &\leq \frac{\kappa^2}{1 - \delta} \mathbb{E}[\mathbf{1}_{-\mathcal{E}} \|\mathbf{P}_{\perp k}\|(\|\mathbf{x}_k\|^2 + \|\boldsymbol{\Sigma}\|)] \leq \frac{\kappa^2}{1 - \delta} (\delta + \mathbb{E}[\mathbf{1}_{-\mathcal{E}} \|\mathbf{x}_k\|^2]). \end{aligned}$$

To analyze the final expectation, we use Euclidean concentration: $\mathbb{P}(\|\mathbf{x}_k\|^2 > t) \leq 2 \exp(-ct/L^2)$ for any $t \geq 2\text{tr}(\boldsymbol{\Sigma}) = 2r$, so:

$$\begin{aligned} \mathbb{E}[\mathbf{1}_{-\mathcal{E}} \|\mathbf{x}_k\|^2] &= \int_0^\infty \mathbb{P}(\mathbf{1}_{-\mathcal{E}} \|\mathbf{x}_k\|^2 > t) dt \leq 2r\delta + \int_{2r}^\infty \mathbb{P}(\|\mathbf{x}_k\|^2 > t) dt \\ &\leq 2r\delta + \int_{2r}^\infty 2 \exp(-ct/L^2) dt \leq CL^2 r \delta, \end{aligned}$$

for some absolute constant $C > 0$. In conclusion, $T_1 \leq \kappa^2(\delta + CL^2 r \delta)/(1 - \delta)$.

3. Bounding T_2 . By Lemma 7, we have

$$\mathbb{E}_{\mathcal{E}}[\mathbf{P}_{\perp k} - \mathbf{P}_{\perp}] = \mathbb{E}_{\mathcal{E}}[\mathbf{P}_{-k} - \mathbf{P}] \leq \mathbb{E}_{\mathcal{E}} \left[\frac{\mathbf{P}_{\perp k} \mathbf{x}_k \mathbf{x}_k^\top \mathbf{P}_{\perp k}}{\mathbf{x}_k^\top \mathbf{P}_{\perp k} \mathbf{x}_k} \right] \leq \frac{4}{r} \cdot \mathbb{E}_{\mathcal{E}}[\mathbf{P}_{\perp k} \boldsymbol{\Sigma} \mathbf{P}_{\perp k}], \quad (27)$$

since, given \mathcal{E} , $\mathbf{x}_k^\top \mathbf{P}_{\perp k} \mathbf{x}_k \geq \frac{1}{2} \text{tr} \boldsymbol{\Sigma} \mathbf{P}_{\perp k} \geq \frac{1}{2}(r - k) \geq r/4$. Also, the spectrum of $\mathbf{P}_{\perp k} \boldsymbol{\Sigma} \mathbf{P}_{\perp k}$ is almost surely bounded as follows:

$$\begin{aligned} \mathbf{P}_{\perp k} \boldsymbol{\Sigma} \mathbf{P}_{\perp k} &= (\mathbf{I} - \mathbf{P}_{-k}) \boldsymbol{\Sigma} (\mathbf{I} - \mathbf{P}_{-k}) \\ &= \boldsymbol{\Sigma} - \mathbf{P}_{-k} \boldsymbol{\Sigma} - \boldsymbol{\Sigma} \mathbf{P}_{-k} + \mathbf{P}_{-k} \boldsymbol{\Sigma} \mathbf{P}_{-k} \\ &\leq \boldsymbol{\Sigma} + \boldsymbol{\Sigma}^2 + \mathbf{P}_{-k}^2 + \mathbf{P}_{-k}^2 \leq 2(\boldsymbol{\Sigma} + \mathbf{P}), \end{aligned} \quad (28)$$

where we used that $\|\boldsymbol{\Sigma}\| = 1$. Observing that $\mathbb{E}_{\mathcal{E}}[\mathbf{P}_{\perp k} - \mathbf{P}_{\perp}] \boldsymbol{\Sigma} \mathbb{E}_{\mathcal{E}}[\mathbf{P}_{\perp k} - \mathbf{P}_{\perp}] \leq \mathbb{E}_{\mathcal{E}}[\mathbf{P}_{\perp k} - \mathbf{P}_{\perp}]$, we get:

$$\begin{aligned} T_2 &= \sqrt{\|\boldsymbol{\Sigma}^{-1/2} \mathbb{E}_{\mathcal{E}}[\mathbf{P}_{\perp k} - \mathbf{P}_{\perp}] \boldsymbol{\Sigma} \mathbb{E}_{\mathcal{E}}[\mathbf{P}_{\perp k} - \mathbf{P}_{\perp}] \boldsymbol{\Sigma}^{-1/2}\|} \\ &\leq \sqrt{\|\boldsymbol{\Sigma}^{-1/2} \mathbb{E}_{\mathcal{E}}[\mathbf{P}_{\perp k} - \mathbf{P}_{\perp}] \boldsymbol{\Sigma}^{-1/2}\|} \\ &\stackrel{(27)}{\leq} \frac{2}{\sqrt{r}} \cdot \sqrt{\|\boldsymbol{\Sigma}^{-1/2} \mathbb{E}_{\mathcal{E}}[\mathbf{P}_{\perp k} \boldsymbol{\Sigma} \mathbf{P}_{\perp k}] \boldsymbol{\Sigma}^{-1/2}\|} \\ &\stackrel{(28)}{\leq} \frac{4}{\sqrt{r}} \cdot \sqrt{\|\boldsymbol{\Sigma}^{-1/2} \mathbb{E}_{\mathcal{E}}[\boldsymbol{\Sigma} + \mathbf{P}] \boldsymbol{\Sigma}^{-1/2}\|} \\ &\leq \frac{C}{\sqrt{r}} \cdot \sqrt{1 + \|\bar{\mathbf{P}}^{-1/2} \mathbb{E}[\mathbf{P}] \bar{\mathbf{P}}^{-1/2}\|} =: \frac{C}{\sqrt{r}} \cdot \sqrt{1 + \rho_1}, \end{aligned}$$

where in the last inequality we used that

$$\Sigma^{-1/2} \leq \sqrt{\gamma} \bar{\mathbf{P}}^{-1/2} \leq \bar{\mathbf{P}}^{-1/2}$$

since $\bar{\mathbf{P}} = \gamma \Sigma (\gamma \Sigma + \mathbf{I})^{-1} \leq \gamma \Sigma$ and $\gamma = k/\mathbb{E} \|\mathbf{A} \mathbf{P}_{\perp k}\|_F^2 \leq k/(r-k) \leq 1$ by the condition on r .

Note the similarity between ρ_1 and ρ . We will return to bounding ρ_1 at the end of the proof, as it requires a recursive argument.

4. Bounding T_3 . First, by Cauchy-Schwartz inequality, letting S^{n-1} denote the unit sphere in \mathbb{R}^n :

$$\begin{aligned} T_3 &= \left\| \mathbb{E}_{\mathcal{E}} \left(\frac{\mathbb{E}\xi - \xi}{\xi} \cdot \Sigma^{-1/2} \mathbf{P}_{\perp k} \mathbf{x}_k \mathbf{x}_k^{\top} \Sigma^{-1/2} \right) \right\| \\ &\leq \sup_{\mathbf{u}, \mathbf{v} \in S^{n-1}} \mathbb{E}_{\mathcal{E}} \left[\frac{|\mathbb{E}\xi - \xi|}{\xi} \cdot \left| \mathbf{v}^{\top} \Sigma^{-1/2} \mathbf{P}_{\perp k} \mathbf{x}_k \mathbf{x}_k^{\top} \Sigma^{-1/2} \mathbf{u} \right| \right] \\ &\leq \sqrt{\mathbb{E}_{\mathcal{E}} \left[\frac{|\mathbb{E}\xi - \xi|^2}{\xi^2} \right]} \cdot \sup_{\mathbf{u}, \mathbf{v} \in S^{n-1}} \sqrt{\mathbb{E}_{\mathcal{E}} \left[(\mathbf{v}^{\top} \Sigma^{-1/2} \mathbf{P}_{\perp k} \mathbf{x}_k \mathbf{x}_k^{\top} \Sigma^{-1/2} \mathbf{u})^2 \right]}. \end{aligned} \quad (29)$$

We estimate these two multiples separately. For the first term in (29), by the definition of the event \mathcal{E} , we have $\xi = \mathbf{x}_k^{\top} \mathbf{P}_{\perp k} \mathbf{x}_k \geq \frac{1}{2} \text{tr}(\Sigma \mathbf{P}_{\perp k})$, so

$$\mathbb{E}_{\mathcal{E}} \left[\frac{|\mathbb{E}\xi - \xi|^2}{(\mathbf{x}_k^{\top} \mathbf{P}_{\perp k} \mathbf{x}_k)^2} \right] \leq \frac{4}{\mathbb{P}(\mathcal{E})} \cdot \mathbb{E} \left[\frac{|\mathbb{E}\xi - \xi|^2}{\text{tr}(\Sigma \mathbf{P}_{\perp k})^2} \right] \leq \frac{4}{1-\delta} \cdot \mathbb{E} \left[\frac{\text{Var}[\mathbf{x}_k^{\top} \mathbf{P}_{\perp k} \mathbf{x}_k \mid \mathbf{P}_{-k}]}{(\text{tr} \Sigma \mathbf{P}_{\perp k})^2} \right].$$

From Lemma 8, we have:

$$\text{Var}[\mathbf{x}_k^{\top} \mathbf{P}_{\perp k} \mathbf{x}_k \mid \mathbf{P}_{-k}] \leq CL^2 \|\mathbf{A} \mathbf{P}_{\perp k}\|^2 (L^2 \|\mathbf{A} \mathbf{P}_{\perp k}\|^2 + \|\mathbf{A} \mathbf{P}_{\perp k}\|_F^2) \leq CL^4 + CL^2 \text{tr} \Sigma \mathbf{P}_{\perp k},$$

so using that $\text{tr} \Sigma \mathbf{P}_{\perp k} \geq r - k$, we obtain:

$$\mathbb{E}_{\mathcal{E}} \left[\left(\frac{\mathbb{E}\xi - \xi}{\xi} \right)^2 \right] \leq 8C \left(\frac{L^4}{(r-k)^2} + \frac{L^2}{r-k} \right) \leq \frac{16CL^2}{r-k}.$$

For the second term in (29), recall that $\mathbf{x}_k = \mathbf{A}^{\top} \mathbf{s}_k$, so, again using Lemma 8 and Cauchy-Schwartz inequality, we have:

$$\begin{aligned} &\mathbb{E}_{\mathcal{E}} \left[(\mathbf{v}^{\top} \Sigma^{-1/2} \mathbf{P}_{\perp k} \mathbf{x}_k \cdot \mathbf{x}_k^{\top} \Sigma^{-1/2} \mathbf{u})^2 \right] \\ &\leq \frac{1}{\mathbb{P}(\mathcal{E})} \mathbb{E} \left[\sqrt{\mathbb{E}[(\mathbf{v}^{\top} \Sigma^{-1/2} \mathbf{P}_{\perp k} \mathbf{A}^{\top} \mathbf{s}_k)^4 \mid \mathbf{P}_{-k}]} \cdot \sqrt{\mathbb{E}[(\mathbf{s}_k^{\top} \mathbf{A} \Sigma^{-1/2} \mathbf{u})^4 \mid \mathbf{P}_{-k}]} \right] \\ &\stackrel{\text{Lemma 8}}{\leq} 2 \mathbb{E} \left[\sqrt{CK^4 \|\mathbf{A} \mathbf{P}_{\perp k} \Sigma^{-1/2} \mathbf{v}\|^4} \cdot \sqrt{CK^4 \|\mathbf{A} \Sigma^{-1/2} \mathbf{u}\|^4} \right] \\ &\leq 2CK^4 \mathbb{E} \left[\mathbf{v}^{\top} \Sigma^{-1/2} \mathbf{P}_{\perp k} \Sigma \mathbf{P}_{\perp k} \Sigma^{-1/2} \mathbf{v} \right], \end{aligned}$$

where we used K -sub-gaussianity of \mathbf{s}_k and the fact that $\|\mathbf{A} \Sigma^{-1/2} \mathbf{u}\| = \|\mathbf{u}\| = 1$. Thus, combining the above with the bound on $\mathbf{P}_{\perp k} \Sigma \mathbf{P}_{\perp k}$ derived earlier in (28), and adjusting the constant C ,

$$\begin{aligned} \sup_{\mathbf{u}, \mathbf{v} \in S^{n-1}} \sqrt{\mathbb{E}_{\mathcal{E}} \left[(\mathbf{v}^{\top} \Sigma^{-1/2} \mathbf{P}_{\perp k} \mathbf{x}_k \mathbf{x}_k^{\top} \Sigma^{-1/2} \mathbf{u})^2 \right]} &\leq \sup_{\mathbf{v} \in S^{n-1}} \sqrt{CK^4 \mathbb{E} \left[\mathbf{v}^{\top} \Sigma^{-1/2} \mathbf{P}_{\perp k} \Sigma \mathbf{P}_{\perp k} \Sigma^{-1/2} \mathbf{v} \right]} \\ &\leq K^2 \sqrt{C \|\Sigma^{-1/2} \mathbb{E}[\mathbf{P}_{\perp k} \Sigma \mathbf{P}_{\perp k}] \Sigma^{-1/2}\|} \\ &\stackrel{(28)}{\leq} K^2 \sqrt{2C(1 + \|\Sigma^{-1/2} \mathbb{E}[\mathbf{P}] \Sigma^{-1/2}\|)} \\ &\leq K^2 \sqrt{2C(1 + \|\bar{\mathbf{P}}^{-1/2} \mathbb{E}[\mathbf{P}] \bar{\mathbf{P}}^{-1/2}\|)}. \end{aligned}$$

As a result, again adjusting C , we conclude that:

$$T_3 \leq C \sqrt{\frac{L^2}{r-k}} \cdot K^2 \sqrt{C(1 + \|\bar{\mathbf{P}}^{-1/2} \mathbb{E}[\mathbf{P}] \bar{\mathbf{P}}^{-1/2}\|)} \leq \frac{CLK^2}{\sqrt{r}} \cdot \sqrt{1 + \rho_1},$$

where $\rho_1 = \|\bar{\mathbf{P}}^{-1/2} \mathbb{E}[\mathbf{P}] \bar{\mathbf{P}}^{-1/2}\|$.

5. Conclusion via a recursive bound. So far, we bounded $\rho_{\mathcal{E}}$ by a quantity ρ_1 that itself depends on ρ , which seems (almost) circular:

$$\rho_{\mathcal{E}} \leq \kappa^2 \delta (1 + C_1 L^2 r) + \frac{C_2}{\sqrt{r}} \sqrt{1 + \rho_1} + \frac{C_3 L K^2}{\sqrt{r}} \cdot \sqrt{1 + \rho_1}. \quad (30)$$

However, together with (26), we have the following relation

$$\begin{aligned} \rho_1 &\leq 1 + \rho \leq 1 + \rho_{\mathcal{E}} + 2(1 + r\kappa^2)\delta \\ &\leq 1 + 2(1 + r\kappa^2)\delta + \kappa^2 \delta (1 + CL^2 r) + \frac{CLK^2}{\sqrt{r}} \cdot \sqrt{1 + \rho_1} \\ &\leq \frac{3}{2} + \frac{1}{2} \sqrt{1 + \rho_1}. \end{aligned}$$

In the last step we used that $r \geq C' \max\{k, L^2 \log \kappa, K^4 L^2\}$ for sufficiently large $C' > 0$ and $\delta = 2 \exp(-cr/L^2)$.

Solving this recursion for ρ_1 , we see that $\rho_1 \leq 3$. Plugging it back to (30), we get that $\rho_{\mathcal{E}} \leq CLK^2/\sqrt{r}$, and through (26) we have that $\rho \leq CLK^2/\sqrt{r}$ with a new constant $C > 0$. This concludes the proof of Theorem 2 by (25). \square

4.3 Sparse sketching: proof of Theorem 3

We will use two results from prior work. The first one shows that a LESS embedding is close in total variation distance to an embedding with strong sub-gaussian concentration. Recall that for random variables X and Y over the same domain, the total variation distance $d_{\text{tv}}(X, Y)$ is the infimum over $\delta > 0$ such that there exists a coupling between X and Y such that $\mathbb{P}(X \neq Y) = \delta$.

Lemma 9 ([Der22]). *Let $\delta \in (0, 1)$. Consider an $m \times n$ matrix \mathbf{A} , where $m \geq n$, and let \mathbf{S} be a LESS embedding matrix for \mathbf{A} with k rows having $O(n \log(nk/\delta))$ non-zeros per row. Then, there is a positive semidefinite matrix $\tilde{\Sigma}$ and a $k \times n$ random matrix \mathbf{Z} with i.i.d. isotropic rows that satisfy both sub-gaussianity and Euclidean concentration with absolute constants, such that:*

$$d_{\text{tv}}(\mathbf{S}\mathbf{A}, \mathbf{Z}\tilde{\Sigma}^{1/2}) \leq \delta \quad \text{and} \quad (1 - \delta)\mathbf{A}^\top \mathbf{A} \leq \tilde{\Sigma} \leq (1 + \delta)\mathbf{A}^\top \mathbf{A}. \quad (31)$$

The second result, which is an immediate corollary of [DLLM20] Theorem 2, gives a precise analytic expression for the expected Randomized SVD error in terms of the singular values of matrix \mathbf{A} .

Lemma 10 ([DLLM20]). *Under the assumptions of Theorem 2, the expected error of Randomized SVD can be approximated by the following implicit analytic expression:*

$$(1 - \epsilon) \cdot k/\bar{\gamma}_k \leq \text{Err}(\mathbf{A}, k-1) \leq (1 + \epsilon) \cdot k/\bar{\gamma}_k \quad \text{for} \quad \epsilon = O(1/\sqrt{r}),$$

where $\bar{\gamma}_k = f^{-1}(k)$, i.e., the function inverse of f at k , for $f(\gamma) = \text{tr} \gamma \Sigma (\gamma \Sigma + \mathbf{I})^{-1}$.

We are now ready to present the proof of Theorem 3. We proceed by comparing the expected projection constructed from $\mathbf{S}\mathbf{A}$ with an analogous expected projection matrix defined by $\mathbf{Z}\tilde{\Sigma}^{1/2}$ (from Lemma 9).

Proof of Theorem 3. We substitute our LESS-embedding projection \mathbf{P} by $\tilde{\mathbf{P}}$ defined via Lemma 9 as:

$$\tilde{\mathbf{P}} := (\mathbf{Z}\tilde{\Sigma}^{1/2})^\dagger \mathbf{Z}\tilde{\Sigma}^{1/2}.$$

First, note that $\tilde{\mathbf{P}}$ satisfies assumptions of Theorem 2: indeed, \mathbf{Z} satisfies the assumptions on the sketching matrix by construction, and both the condition number κ and the stable rank r of $\tilde{\Sigma}^{1/2}$ are within a factor of $(1 \pm \delta)$ of the corresponding quantities for \mathbf{A} by (31). So, they satisfy the required mutual relations, potentially with slightly different absolute constants. Thus, combining the estimates from Theorem 2 and Lemma 10, we have

$$(1 - \tilde{\epsilon})\tilde{\gamma}_k\tilde{\Sigma}(\tilde{\gamma}_k\tilde{\Sigma} + \mathbf{I})^{-1} \leq \mathbb{E}[\tilde{\mathbf{P}}] \leq (1 + \tilde{\epsilon})\tilde{\gamma}_k\tilde{\Sigma}(\tilde{\gamma}_k\tilde{\Sigma} + \mathbf{I})^{-1} \quad \text{for } \tilde{\epsilon} = O(1/\sqrt{r}), \quad (32)$$

where $\tilde{\gamma}_k = \tilde{f}^{-1}(k)$, with $\tilde{f}(\gamma) = \text{tr} \gamma \tilde{\Sigma}(\gamma \tilde{\Sigma} + \mathbf{I})^{-1}$. Our goal is to show that $\mathbb{E}[\mathbf{P}]$ and its respective surrogate expression $\tilde{\gamma}_k\tilde{\Sigma}(\tilde{\gamma}_k\tilde{\Sigma} + \mathbf{I})^{-1}$ satisfy the same mutual relationship (32) with $\epsilon \leq C\tilde{\epsilon}$. We will do this in two steps: first, we estimate $\mathbb{E}[\mathbf{P}]$ via new surrogates coming from (32), and then, we show that the two surrogate expressions are close.

Step 1. Since \mathbf{SA} and $\mathbf{Z}\tilde{\Sigma}^{1/2}$ are within δ total variation distance, we can couple these two random matrices so that the event $\mathcal{E} := \{\mathbf{P} = \tilde{\mathbf{P}}\}$ holds with probability $1 - \delta$. We observe that since $\tilde{\gamma}_k \geq k/\text{tr}(\tilde{\Sigma}) \geq k/n$, we have $\lambda_{\min}(\tilde{\gamma}_k\tilde{\Sigma}(\tilde{\gamma}_k\tilde{\Sigma} + \mathbf{I})^{-1}) = \lambda_{\max}^{-1}(\mathbf{I} + \tilde{\gamma}_k^{-1}\tilde{\Sigma}^{-1}) \geq k/(2n\kappa^2)$. As a result, letting $\delta \leq \epsilon/(n\kappa^2)$,

$$\begin{aligned} \mathbb{E}[\mathbf{P}] &= \mathbb{P}(\mathcal{E})\mathbb{E}[\mathbf{P} \mid \mathcal{E}] + \mathbb{P}(-\mathcal{E})\mathbb{E}[\mathbf{P} \mid -\mathcal{E}] \\ &\geq \mathbb{P}(\mathcal{E})\mathbb{E}[\tilde{\mathbf{P}} \mid \mathcal{E}] \\ &= \mathbb{E}[\tilde{\mathbf{P}}] - \mathbb{P}(-\mathcal{E})\mathbb{E}[\tilde{\mathbf{P}} \mid -\mathcal{E}] \\ &\geq \mathbb{E}[\tilde{\mathbf{P}}] - \delta\mathbf{I} \\ &\geq \mathbb{E}[\tilde{\mathbf{P}}] - \frac{\epsilon}{n\kappa^2} \cdot 2n\kappa^2 \tilde{\gamma}_k\tilde{\Sigma}(\tilde{\gamma}_k\tilde{\Sigma} + \mathbf{I})^{-1} \\ &\geq (1 - 3\epsilon)\tilde{\gamma}_k\tilde{\Sigma}(\tilde{\gamma}_k\tilde{\Sigma} + \mathbf{I})^{-1}, \end{aligned}$$

and on the other side, analogously we obtain:

$$\mathbb{E}[\mathbf{P}] = \mathbb{P}(\mathcal{E})\mathbb{E}[\mathbf{P} \mid \mathcal{E}] + \mathbb{P}(-\mathcal{E})\mathbb{E}[\mathbf{P} \mid -\mathcal{E}] \leq \mathbb{P}(\mathcal{E})\mathbb{E}[\tilde{\mathbf{P}} \mid \mathcal{E}] + \delta\mathbf{I} \leq (1 + 3\epsilon)\tilde{\gamma}_k\tilde{\Sigma}(\tilde{\gamma}_k\tilde{\Sigma} + \mathbf{I})^{-1}.$$

This way, we estimated $\mathbb{E}[\mathbf{P}]$ via the approximated surrogate $\tilde{\gamma}_k\tilde{\Sigma}(\tilde{\gamma}_k\tilde{\Sigma} + \mathbf{I})^{-1}$.

Step 2. It remains to show that $\tilde{\gamma}_k\tilde{\Sigma}(\tilde{\gamma}_k\tilde{\Sigma} + \mathbf{I})^{-1}$ is close to $\tilde{\gamma}_k\tilde{\Sigma}(\tilde{\gamma}_k\tilde{\Sigma} + \mathbf{I})^{-1}$, for $\tilde{\gamma}_k = f^{-1}(k)$, with $f(\gamma) = \text{tr} \gamma \tilde{\Sigma}(\gamma \tilde{\Sigma} + \mathbf{I})^{-1}$. After that, we can conclude Theorem 3 with $\gamma_k = k/\text{Err}(\mathbf{A}, k - 1)$ by using Lemma 10 again.

Further, it is enough to compare $\tilde{\gamma}_k$ and $\tilde{\gamma}_k$ since we know that $\tilde{\Sigma}$ is a $(1 \pm \delta)$ -approximation of Σ (31). Another consequence of $\tilde{\Sigma}$ and Σ being δ -close is that $\tilde{\gamma}_k = f^{-1}(\tilde{k})$ for some \tilde{k} being a $(1 \pm \delta)$ -approximation of k . Thus, it suffices to show that $f^{-1}(\tilde{k}) \approx f^{-1}(k)$ for

$$f(\gamma) = \text{tr} \gamma \tilde{\Sigma}(\gamma \tilde{\Sigma} + \mathbf{I})^{-1} \quad \text{and any } \tilde{k} : |k - \tilde{k}| \leq \delta k.$$

We show this by bounding the derivative of f^{-1} at any point in $[0, r/2]$ (which includes both k and \tilde{k}), and then relying on the mean value theorem. First, let $\sigma_1, \sigma_2, \dots$ be the decreasing singular values of \mathbf{A} , and assume without loss of generality that $\sigma_1 = 1$. Observe that

$$f(\gamma) = \sum_i \frac{\gamma \sigma_i^2}{\gamma \sigma_i^2 + 1} \geq \frac{\gamma \sum_i \sigma_i^2}{\gamma \sigma_1^2 + 1} = \frac{\gamma r}{\gamma + 1},$$

so $f^{-1}(x) = \gamma \leq \frac{x}{r-x} \leq 1$ for $x \leq r/2$. This holds for k, \tilde{k} and any value in between, so we can compute

$$f'(\gamma) = \frac{d}{d\gamma} \left(\sum_i \frac{\gamma \sigma_i^2}{\gamma \sigma_i^2 + 1} \right) = \sum_i \frac{\sigma_i^2}{(\gamma \sigma_i^2 + 1)^2} \geq \frac{1}{4} \sum_i \sigma_i^2 = \frac{r}{4} \quad \text{and} \quad \frac{df^{-1}(x)}{dx} = \frac{1}{f'(f^{-1}(x))} \leq \frac{4}{r}.$$

Now, by the mean value theorem:

$$|\tilde{\gamma}_k - \bar{\gamma}_k| = |f^{-1}(\tilde{k}) - f^{-1}(k)| \leq \frac{4}{r} \cdot |k - \tilde{k}| \leq 4\delta \cdot \frac{k}{r} \leq 4\delta \cdot \bar{\gamma}_k,$$

where the last step follows because

$$k = \sum_i \frac{\tilde{\gamma}_k \sigma_i^2}{\tilde{\gamma}_k \sigma_i^2 + 1} \leq \tilde{\gamma}_k \sum_i \sigma_i^2 = \tilde{\gamma}_k r.$$

Thus, we have that $\tilde{\gamma}_k$ and $\bar{\gamma}_k$ are within $1 + O(\delta)$ factor to each other, thus two surrogate expressions are similarly close to each other and Step 2 is concluded. This concludes the proof of Theorem 3 with $\epsilon = 2n\kappa^2\delta$ and

$$O(n \log(nk/\delta)) = O(n \log(nk\kappa/\epsilon)) = O(n \log(nk\kappa r)) = O(n \log(n\kappa))$$

non-zero entries per row of the sketching matrix. \square

5 Experiments

In this section, our goal is to provide additional support for our theoretical bounds and to demonstrate how the new bounds can inform us about the optimal sketch sizes and sparsity levels when using sketch-and-project methods. In Sections 5.1 and 5.2, we test the Block Gaussian Kaczmarz method (assuming $\mathbf{B} = \mathbf{I}$ throughout) with various sketch sizes k . Then, in Section 5.3, we replace the Gaussian sketching matrix with LESS-based sparse sketching matrices, varying their sparsity. We consider artificial linear problems, as well as matrices coming from real-world datasets.

The artificial matrices have dimensions 5000×150 , and are generated to have various spectral profiles. It is done in the following way. Initial SVD decomposition $\mathbf{A} = \mathbf{U}\mathbf{\Sigma}\mathbf{V}$ is constructed for a standard Gaussian matrix \mathbf{A} with the rows normalized to have unit norm. Such matrix has almost linear spectral decay and well-conditioned smallest singular value (diagonal entries of $\mathbf{\Sigma}$ roughly span the segment $[6.8, 4.8]$). Based on that, we substitute $\mathbf{\Sigma}$ with artificial diagonal matrices having the following spectral decays. Models 'lin.01', 'lin.025' and 'lin.035' are the matrices $\mathbf{U}\bar{\mathbf{\Sigma}}\mathbf{V}$ with the entries of $\bar{\mathbf{\Sigma}}$ having linear decays $\sigma_i = 6.8 - l \cdot i$ with $l = 0.01, 0.025$, and 0.035 (which results in σ_{\min} being 5.3, 3.1 and 1.6, respectively). Two polynomial decay models 'poly1' and 'poly1.5' are imposed by the entries of $\bar{\mathbf{\Sigma}}$ defined by $\sigma_i = 6.8 i^{-l}$, for $l = 1$ and $l = 1.5$ respectively. Finally, in 'step20' model, $\bar{\mathbf{\Sigma}}$ has its 20 top singular values the same as in 'lin.01' model and the rest are as in 'poly1' model, and 'step37' model does the same transition from linear to polynomial decay at the 37-th singular value. Note that all models are constructed to share the same largest singular value, so that the smallest singular value is the correct indicator of how well-conditioned the system is.

We also consider three other data matrices: a 5000×150 random matrix with entries randomly generated i.i.d. $N(0,1)$ and then normalized to have unit length rows ('gaus'); a 1280×256 sub-matrix of the USPS dataset [CL11] ('usps'); a 1500×300 sub-matrix of the w8a-X dataset [CL11] ('w8a'). We note that 'w8a' is not a full-rank dataset, so the convergence error is computed with respect to the least squares solution, which randomized Kaczmarz is known to converge to on rank-deficient systems [ZF13].

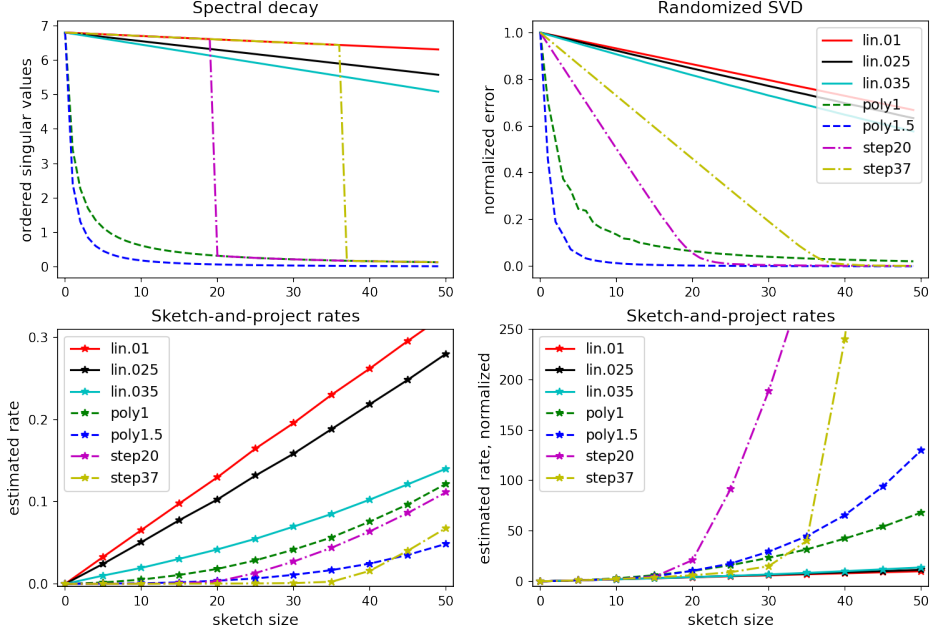


Figure 1: Bottom left figure shows the estimated convergence rates computed as in (33) (larger is better), showing that linear decays result in faster convergence in general due to having larger smallest singular value. However, the normalized version of the same plot on bottom right demonstrates that the relative speed-up with increased sketch size is quicker for polynomial spectral decays, shadowing the claim of Corollary 1 (polynomial rate growth on polynomial spectra) and Corollary 2 (inverse to the profiles of Randomized SVD error). Normalized randomized SVD error is computed as $\|\mathbf{A}(\mathbf{I} - \mathbf{P})\|_F / \|\mathbf{A}\|_F$ (top right, smaller is better).

5.1 Sketch size and convergence

In Figure 1, we demonstrate the scaling of the estimated convergence rate with the sketch size k . In particular, we show that linear spectral decays result in linear per-iteration speed up with growing sketch size, whereas quicker (polynomial) spectral decays result in accelerated rate improvement with sketch size. Moreover, we demonstrate the similarity between the error of Randomized SVD (8) and the convergence speed-up of sketch-and-project: when the spectral decay has an abrupt change at i -th ordered singular value, then about i components are needed for a small error in Randomized SVD, and similarly, sketch sizes $k \geq i$ drive efficient convergence of the iterative solver.

The estimated expected convergence rate is computed as the mean of

$$1 - \frac{\|\mathbf{x}_t - \mathbf{x}_*\|^2}{\|\mathbf{x}_{t-1} - \mathbf{x}_*\|^2} \sim \text{Rate}(\mathbf{A}, k) \quad (33)$$

over the last 50 iterations in 100 runs (recall that initially the randomized Kaczmarz method exhibits an accelerated convergence rate depending on full spectrum of the matrix, and we aim to show the “limiting” rate after stabilization). We run the method for 1000 iterations or until $\|\mathbf{x}_t - \mathbf{x}_*\| < 10^{-5}$. We estimate the expected rate for the sketch sizes $k = 5j$ for $j = 1, \dots, 10$.

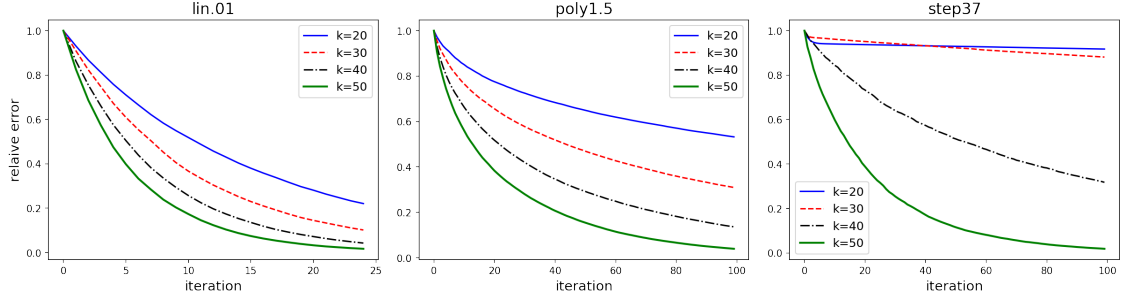


Figure 2: Per iteration convergence for various artificial models and various sketch sizes k . Polynomial model results in substantial improvements as sketch size grows, and the linear model convergence improves less with the growing sketch size. For the step singular values decay, we see a threshold: having the sketch size bigger than the number of "large" singular values (approximate rank) drives an effective convergence rate.

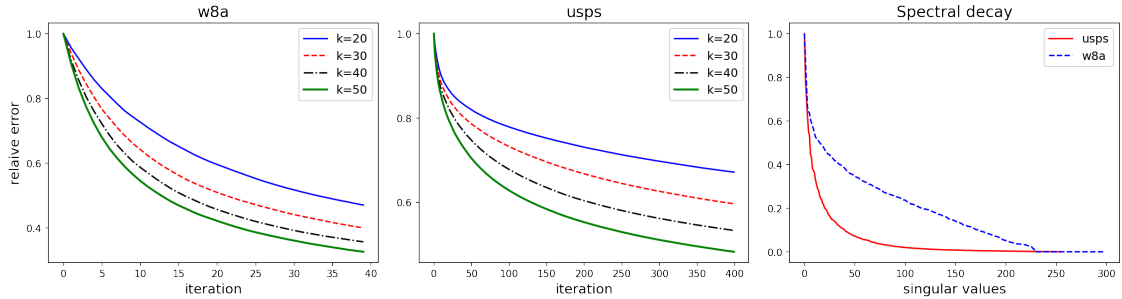


Figure 3: Per iteration convergence for two models based on real-world data matrices \mathbf{A} (left and middle) and their spectral profiles (right). Sketch size is equal to k . A real-world dataset with more "linear" spectral decay ('w8a') shows less convergence improvement with bigger sketch sizes.

In Figure 1 (bottom left), we see that linear models are generally the fastest to converge. This is not surprising as they are the best conditioned (having smallest singular values above 1.5). To emphasize the relationship between the rate and the sketch size, in Figure 1 (bottom right), we normalize the rates by the first non-trivial point, the rate at $k = 5$. We can see that the acceleration of the rate for linear models is the slowest, and that 'step' models spike with the behavior roughly reverse to their Randomized SVD error, as plotted in Figure 1 (top right).

In Figures 2 and 3, we also show how sketch size influences the convergence behavior of sketched Kaczmarz, depending on the dataset, by plotting relative error after a certain number of iterations. The relative error after t steps is computed as $\|\mathbf{x}_t - \mathbf{x}_*\|/\|\mathbf{x}_*\|$. Our initial guess \mathbf{x}_0 is all zeros vector. We demonstrate that faster polynomial spectral decay (Figure 2 middle) means better improvement of the convergence speed with growing k , compared to the slower linear spectral decay (Figure 2 left). Similar effect is observed on real-world datasets (Figure 3): the spectral decay of 'w8a' is flatter than the spectrum of 'usps', and increasing the sketch size k makes less significant improvement of convergence speed.

5.2 Theoretical bounds

In Figure 4, we show a comparison between the estimated expected convergence rate and the theoretical lower bounds, on the artificial data matrices.

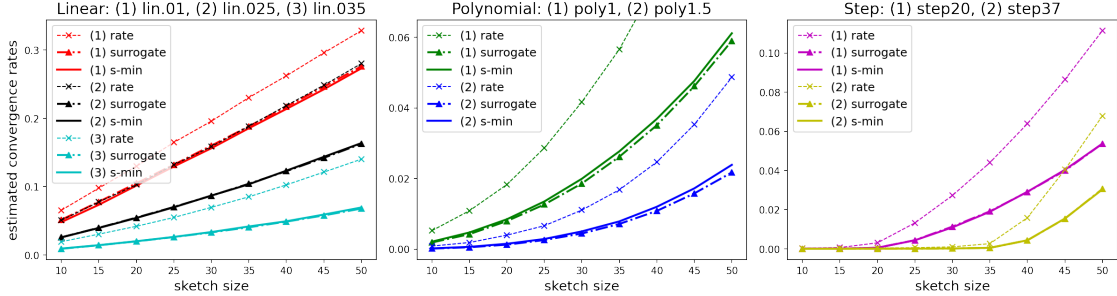


Figure 4: As claimed by Theorem 2, our surrogate expression computed as in (34), is a very tight estimator for s-min := $\lambda_{\min}(\mathbb{E}[\mathbf{P}])$. Both quantities lower bound and mimic the convergence rate of sketch-and-project (larger rate is better).

As the theoretical bounds, we show: (a) 's-min': $\lambda_{\min}(\mathbb{E}[\mathbf{P}])$, i.e., the classical lower bound (5) (coming from [GR15]), estimated as the smallest eigenvalue of the mean of 1600 sampled projection matrices; and (b) 'surrogate': our new surrogate estimate for $\lambda_{\min}(\mathbb{E}[\mathbf{P}])$ (from Corollary 2), defined via the Randomized SVD error:

$$\frac{k\sigma_{\min}^2(\mathbf{A})}{k\sigma_{\min}^2(\mathbf{A}) + \mathbb{E}\|\mathbf{A}(\mathbf{I} - \mathbf{P}^{(k-1)})\|_F^2}, \quad (34)$$

where $\mathbf{P}^{(k-1)} = (\mathbf{S}^{(k-1)}\mathbf{A})^\dagger\mathbf{S}^{(k-1)}\mathbf{A}$ and the expectation is estimated as a mean over 50 Gaussian $(k-1) \times m$ sketches $\mathbf{S}^{(k-1)}$. We see that the two theoretical bounds 's-min' and 'surrogate' are very close to each other (in most cases, they are difficult to tell apart), which confirms that there is very little slack in our main results (i.e., ϵ from Theorem 2 is very close to 0 in practice). Furthermore, they both lower-bound and effectively mimic the shape of the empirical convergence rate curve, as we vary the sketch size k . We note that the remaining gap between the rate and the bounds is primarily due to the slack in the classical inequality relating the rate and $\lambda_{\min}(\mathbb{E}[\mathbf{P}])$, so it is entirely independent of our analysis.

5.3 Sparse sketching and convergence

In Figure 5, we show that sketches formed with extremely sparse matrices \mathbf{S} usually exhibit very similar convergence behavior to a dense Gaussian \mathbf{S} .

In our experiments, the sparsity level is controlled by the number of non-zeros per row of sketching matrix \mathbf{S} (smaller number means sparser matrix). The non-zero entries of \mathbf{S} are Gaussian, and chosen uniformly at random, which corresponds to a simplified version of LESS embeddings, called LessUniform [DLPM21]. For a highly coherent dataset one might consider to pre-process the data with a randomized Fourier transform, as discussed in Section 2.3. Clearly, sparse sketching matrices can be stored and applied much faster than dense ones: a $k \times m$ sketching matrix \mathbf{S} with s non-zeros per row requires $O(ks)$ memory and $O(ksn)$ time to apply to an $m \times n$ matrix \mathbf{A} . However, efficient implementation of sparse computations is out of the scope of this paper.

Specifically, we compare the relative error after 30 steps of the algorithm for several sketch sizes and sparsity regimes. We observe that even sketches with extremely sparse matrix \mathbf{S} can lead to a convergence that is nearly as fast as in the dense Gaussian case. Only for some real-world datasets, we observe some degradation in performance as we get close to 1-sparse sketching matrices (i.e., one non-zero per row). This suggests that the $O(n \log n)$ non-zeros per row required by our theory (Theorem 3) is very conservative.

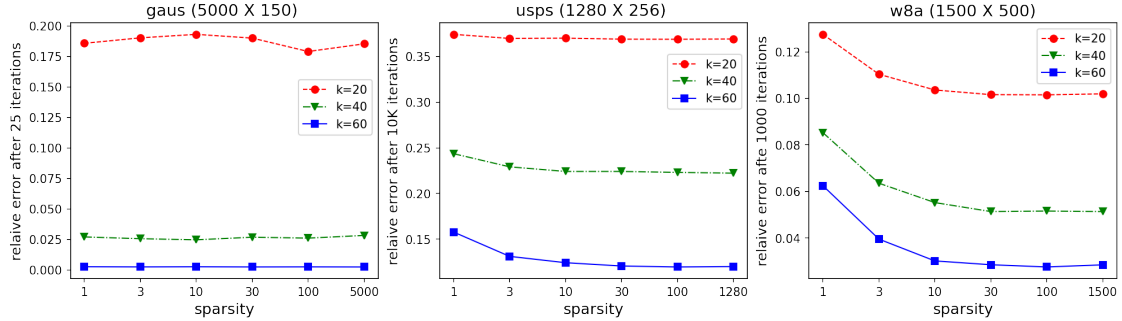


Figure 5: Relative error after the same number of iterations for dense and sparse sketching matrices \mathbf{S} , averaged over 30 runs (smaller is better). Sparsity is the number of non-zeros per row of \mathbf{S} : the rightmost point refers to the dense case and the leftmost point is for extreme sparsity. We observe consistency of performance between dense and significantly sparse matrices \mathbf{S} . For Gaussian data, 1-sparse \mathbf{S} (that effectively performs row sampling) have the performance identical to the dense \mathbf{S} . However, depending on the dataset, extremely sparse \mathbf{S} can lead to slower convergence.

We note that 1-sparse sketching matrices are equivalent to block sketching via row sampling since multiplying by a Gaussian scalar does not change a subspace associated with a particular equation hyperplane. In the Kaczmarz case, it is the same as a randomized block Kaczmarz version with randomly sampled rows (as discussed in [HM21]). Even though the 1-sparse case is not covered by our theory, one can hypothesize that general trends, such as scaling with the sketch size, can be estimated for cost-efficient block sketching from the results for LESS sketches.

6 Conclusions and future directions

In this work, we give new sharper bounds for the convergence rate of iterative solvers based on the sketch-and-project framework, via a discovered connection between the convergence rate of sketch-and-project and the approximation error of Randomized SVD, a family of popular sketching-based matrix approximation algorithms. This way, we also connect two classical and seemingly unrelated applications of sketching. Our main technical contribution is providing a new spectral analysis of expected projections onto the span of random matrices that arise from sketching.

We conjecture that our assumptions on the stable rank and condition number in Theorem 2 (full-spectrum analysis of the expected projection) can be relaxed, and we leave this as an open question for future work. Further extensions of our analysis could include quantifying the initial phase of the accelerated convergence, as well as a sharp analysis of sketch-and-project for noisy or under-determined linear systems.

More broadly, our results give rise to many potential future directions. First, given the new connection between sketch-and-project and Randomized SVD, it is natural to ask whether recent algorithmic developments in sketching-based matrix approximation (see [MT20] for an overview) can inspire new iterative solvers and extensions of sketch-and-project. Furthermore, expected projections also find applications in machine learning and statistics, for example in the analysis of random feature models [Bac17], density estimation [SGSS07], Gaussian processes [BRVDW19], kernel mean embeddings [MFSS17], numerical integration algorithms [BBC19], and more. Extending our results to these applications is a promising direction for future work.

References

- [AC09] Nir Ailon and Bernard Chazelle. The fast johnson–lindenstrauss transform and approximate nearest neighbors. *SIAM Journal on computing*, 39(1):302–322, 2009.
- [Agm54] Shmuel Agmon. The relaxation method for linear inequalities. *Canadian Journal of Mathematics*, 6:382–392, 1954.
- [Bac17] Francis Bach. On the equivalence between kernel quadrature rules and random feature expansions. *The Journal of Machine Learning Research*, 18(1):714–751, 2017.
- [BBC19] Ayoub Belhadji, Rémi Bardenet, and Pierre Chainais. Kernel quadrature with dpps. In *Advances in Neural Information Processing Systems*, pages 12927–12937, 2019.
- [BMD08] Christos Boutsidis, Michael Mahoney, and Petros Drineas. An improved approximation algorithm for the column subset selection problem. *Proceedings of the Annual ACM-SIAM Symposium on Discrete Algorithms*, 12 2008.
- [BN15] Jonathan Briskman and Deanna Needell. Block Kaczmarz method with inequalities. *Journal of Mathematical Imaging and Vision*, 52(3):385–396, 2015.
- [BRVDW19] David Burt, Carl Edward Rasmussen, and Mark Van Der Wilk. Rates of convergence for sparse variational Gaussian process regression. In Kamalika Chaudhuri and Ruslan Salakhutdinov, editors, *Proceedings of the 36th International Conference on Machine Learning*, volume 97 of *Proceedings of Machine Learning Research*, pages 862–871, Long Beach, California, USA, 09–15 Jun 2019. PMLR.
- [BV04] Stephen Boyd and Lieven Vandenberghe. *Convex optimization*. Cambridge university press, 2004.
- [CDV20] Daniele Calandriello, Michał Dereziński, and Michal Valko. Sampling from a k -DPP without looking at all items. In *Advances in Neural Information Processing Systems*, volume 33, pages 6889–6899, 2020.
- [CF11] R. Dennis Cook and Liliana Forzani. On the mean and variance of the generalized inverse of a singular wishart matrix. *Electron. J. Statist.*, 5:146–158, 2011.
- [CL11] Chih-Chung Chang and Chih-Jen Lin. Libsvm: A library for support vector machines. *ACM transactions on intelligent systems and technology (TIST)*, 2(3):1–27, 2011.
- [CW17] Kenneth L. Clarkson and David P. Woodruff. Low-rank approximation and regression in input sparsity time. *J. ACM*, 63(6):54:1–54:45, January 2017.
- [Der19] Michał Dereziński. Fast determinantal point processes via distortion-free intermediate sampling. In *Proceedings of the Thirty-Second Conference on Learning Theory*, pages 1029–1049, 2019.
- [Der22] Michał Dereziński. Algorithmic gaussianization through sketching: Converting data into sub-gaussian random designs. *arXiv preprint arXiv:2206.10291*, 2022.
- [DKM20] Michał Dereziński, Rajiv Khanna, and Michael W Mahoney. Improved guarantees and a multiple-descent curve for Column Subset Selection and the Nyström method. In *Advances in Neural Information Processing Systems*, volume 33, pages 4953–4964, 2020.
- [DLDM21] Michał Dereziński, Zhenyu Liao, Edgar Dobriban, and Michael W Mahoney. Sparse sketches with small inversion bias. In *Proceedings of the 34th Conference on Learning Theory*, 2021.

- [DLHN17] Jesus A De Loera, Jamie Haddock, and Deanna Needell. A sampling Kaczmarz–Motzkin algorithm for linear feasibility. *SIAM Journal on Scientific Computing*, 39(5):S66–S87, 2017.
- [DLLM20] Michał Dereziński, Feynman Liang, Zhenyu Liao, and Michael W Mahoney. Precise expressions for random projections: Low-rank approximation and randomized Newton. In *Advances in Neural Information Processing Systems*, volume 33, pages 18272–18283, 2020.
- [DLM20] Michał Dereziński, Feynman Liang, and Michael W Mahoney. Exact expressions for double descent and implicit regularization via surrogate random design. In *Advances in Neural Information Processing Systems*, volume 33, pages 5152–5164, 2020.
- [DLPM21] Michał Dereziński, Jonathan Lacotte, Mert Pilanci, and Michael W Mahoney. Newton-LESS: Sparsification without trade-offs for the sketched newton update. *Advances in Neural Information Processing Systems*, 34:2835–2847, 2021.
- [DM21] Michał Dereziński and Michael W Mahoney. Determinantal point processes in randomized numerical linear algebra. *Notices of the American Mathematical Society*, 68(1):34–45, 2021.
- [DMIMW12] Petros Drineas, Malik Magdon-Ismail, Michael W. Mahoney, and David P. Woodruff. Fast approximation of matrix coherence and statistical leverage. *Journal of Machine Learning Research*, 13:3475–3506, 2012.
- [DS01] Kenneth R Davidson and Stanislaw J Szarek. Local operator theory, random matrices and Banach spaces. *Handbook of the geometry of Banach spaces*, 1(317–366):131, 2001.
- [GKLR19] Robert Gower, Dmitry Koralev, Felix Lieder, and Peter Richtarik. RSN: Randomized subspace Newton. In H. Wallach, H. Larochelle, A. Beygelzimer, F. d Alché-Buc, E. Fox, and R. Garnett, editors, *Advances in Neural Information Processing Systems 32*, pages 614–623. Curran Associates, Inc., 2019.
- [GMMN21] Robert M Gower, Denali Molitor, Jacob Moorman, and Deanna Needell. On adaptive sketch-and-project for solving linear systems. *SIAM Journal on Matrix Analysis and Applications*, 42(2):954–989, 2021.
- [GR15] Robert M. Gower and Peter Richtárik. Randomized iterative methods for linear systems. *SIAM. J. Matrix Anal. & Appl.*, 36(4), 1660–1690, 2015, 2015.
- [GR17] Robert M Gower and Peter Richtárik. Randomized quasi-Newton updates are linearly convergent matrix inversion algorithms. *SIAM Journal on Matrix Analysis and Applications*, 38(4):1380–1409, 2017.
- [HDNR20] Filip Hanzely, Nikita Doikov, Yurii Nesterov, and Peter Richtarik. Stochastic subspace cubic Newton method. In *International Conference on Machine Learning*, pages 4027–4038. PMLR, 2020.
- [HKZ⁺12] Daniel Hsu, Sham Kakade, Tong Zhang, et al. A tail inequality for quadratic forms of subgaussian random vectors. *Electronic Communications in Probability*, 17, 2012.
- [HM21] Jamie Haddock and Anna Ma. Greed works: An improved analysis of sampling Kaczmarz–Motzkin. *SIAM Journal on Mathematics of Data Science*, 3(1):342–368, 2021.
- [HMRT19] T. Hastie, A. Montanari, S. Rosset, and R. J. Tibshirani. Surprises in high-dimensional ridgeless least squares interpolation. Technical Report Preprint: arXiv:1903.08560, 2019.

- [HMT11] Nathan Halko, Per-Gunnar Martinsson, and Joel A Tropp. Finding structure with randomness: Probabilistic algorithms for constructing approximate matrix decompositions. *SIAM review*, 53(2):217–288, 2011.
- [Its07] Mikhail Itskov. *Tensor algebra and tensor analysis for engineers*. Springer, 2007.
- [Kac37] Stefan Kaczmarz. Angenaherte auflosung von systemen linearer gleichungen. *Bull. Int. Acad. Pol. Sic. Let., Cl. Sci. Math. Nat.*, pages 355–357, 1937.
- [LL10] Dennis Leventhal and Adrian S Lewis. Randomized methods for linear constraints: convergence rates and conditioning. *Mathematics of Operations Research*, 35(3):641–654, 2010.
- [MDK20] Mojmir Mutny, Michał Dereziński, and Andreas Krause. Convergence analysis of block coordinate algorithms with determinantal sampling. In *International Conference on Artificial Intelligence and Statistics*, pages 3110–3120, 2020.
- [Mey73] Carl D. Meyer. Generalized inversion of modified matrices. *SIAM Journal on Applied Mathematics*, 24(3):315–323, 1973.
- [MFSS17] K Muandet, K Fukumizu, B Sriperumbudur, and B Schölkopf. Kernel mean embedding of distributions: A review and beyond. *Foundations and Trends in Machine Learning*, 10(1-2):1–144, 2017.
- [MT20] Per-Gunnar Martinsson and Joel A Tropp. Randomized numerical linear algebra: Foundations and algorithms. *Acta Numerica*, 29:403–572, 2020.
- [NN13] Jelani Nelson and Huy L. Nguyên. Osnap: Faster numerical linear algebra algorithms via sparser subspace embeddings. In *Proceedings of the 2013 IEEE 54th Annual Symposium on Foundations of Computer Science, FOCS '13*, pages 117–126, Washington, DC, USA, 2013. IEEE Computer Society.
- [NT14] Deanna Needell and Joel A Tropp. Paved with good intentions: analysis of a randomized block Kaczmarz method. *Linear Algebra and its Applications*, 441:199–221, 2014.
- [NT21] Ion Necoara and Martin Takác. Randomized sketch descent methods for non-separable linearly constrained optimization. *IMA Journal of Numerical Analysis*, 41(2):1056–1092, 2021.
- [NW13] Deanna Needell and Rachel Ward. Two-subspace projection method for coherent overdetermined systems. *Journal of Fourier Analysis and Applications*, 19(2):256–269, 2013.
- [RK20] Anton Rodomanov and Dmitry Kropotov. A randomized coordinate descent method with volume sampling. *SIAM Journal on Optimization*, 30(3):1878–1904, 2020.
- [RN19] Elizaveta Rebrova and Deanna Needell. Sketching for Motzkin’s iterative method for linear systems. In *2019 53rd Asilomar Conference on Signals, Systems, and Computers*, pages 271–275. IEEE, 2019.
- [RN21] Elizaveta Rebrova and Deanna Needell. On block Gaussian sketching for the Kaczmarz method. *Numerical Algorithms*, 86(1):443–473, 2021.
- [RV13] Mark Rudelson and Roman Vershynin. Hanson-Wright inequality and sub-gaussian concentration. *Electronic Communications in Probability*, 18, 2013.
- [SB95] Jack W Silverstein and ZD Bai. On the empirical distribution of eigenvalues of a class of large dimensional random matrices. *Journal of Multivariate analysis*, 54(2):175–192, 1995.

- [SGSS07] Alex Smola, Arthur Gretton, Le Song, and Bernhard Schölkopf. A hilbert space embedding for distributions. In *International Conference on Algorithmic Learning Theory*, pages 13–31. Springer, 2007.
- [Ste21] Stefan Steinerberger. Randomized Kaczmarz converges along small singular vectors. *SIAM Journal on Matrix Analysis and Applications*, 42(2):608–615, 2021.
- [SV09] Thomas Strohmer and Roman Vershynin. A randomized Kaczmarz algorithm with exponential convergence. *Journal of Fourier Analysis and Applications*, 15(2):262–278, 2009.
- [Tro11] Joel A Tropp. Improved analysis of the subsampled randomized hadamard transform. *Advances in Adaptive Data Analysis*, 3(01n02):115–126, 2011.
- [Woo14] David P Woodruff. Sketching as a tool for numerical linear algebra. *arXiv preprint arXiv:1411.4357*, 2014.
- [YLG22] Rui Yuan, Alessandro Lazaric, and Robert M Gower. Sketched Newton–Raphson. *SIAM Journal on Optimization*, 32(3):1555–1583, 2022.
- [ZF13] Anastasios Zouzias and Nikolaos M Freris. Randomized extended kaczmarz for solving least squares. *SIAM Journal on Matrix Analysis and Applications*, 34(2):773–793, 2013.